JGR Atmospheres

RESEARCH ARTICLE
10.1029/2024JD042963

Constraining Future Projections of Freezing Level Height and Equilibrium-Line Altitudes in the Tropical Andes Based on CMIP6

Shelby A. Turner[1,2], Mathias Vuille[1], and Antoine Rabatel[3]

[1]Department of Atmospheric & Environmental Sciences, University at Albany, Albany, NY, USA, [2]Department of Earth, Atmosphere, and Environment, Northern Illinois University, DeKalb, IL, USA, [3]University Grenoble Alpes, CNRS, IRD, INRAE, Grenoble-INP, Institut des Géosciences de l'Environnement (IGE, UMR 5001), Grenoble, France

Abstract Over the past several decades, glacier retreat in the tropical Andes has accelerated. Given the role glacier melt plays for water supply, ecosystem integrity and glacier-related natural hazards, improving projections of glacier changes in the region is critical. The accuracy of global climate models in this region remains an issue as the complex terrain and climate characteristics are difficult to realistically simulate. Here, we examine historical changes of freezing level height (FLH) on four tropical Andean glaciers: Antisana 15 glacier in Ecuador, Artesonraju glacier and Quelccaya ice cap in Peru, and Zongo glacier in Bolivia. The changes in FLH at each site are estimated based on ERA5 reanalysis data and then compared with historical simulations from 35 different CMIP6 models. Constraints are then placed on future projections via correction of model bias, selection of "best-performing" models, and excluding models with an equilibrium climate sensitivity outside the Intergovernmental Panel on Climate Change AR6 likely range. By utilizing the significant empirical linear relationship observed between FLH and glacier equilibrium-line altitude, we estimate the future shrinkage of the glaciers' accumulation zone under two emissions scenarios, SSP2-4.5 and SSP5-8.5. By the year 2100, the Quelccaya ice cap will likely have passed a point of no return, committing to losing its entire accumulation zone, regardless of emission pathway. The same is true for Antisana 15-alpha glacier under SSP5-8.5 while a small accumulation zone remains under SSP2-4.5. Thanks to their higher accumulation area, Zongo and Artesonraju glaciers are more likely to survive beyond 2100, albeit in a strongly reduced extent.

Plain Language Summary Glaciers are visible indicators of the effects of climate change throughout the globe, with tropical glaciers being especially sensitive to changes in climate. The portion of the Andes mountains located in the tropics contains more than 99% of the world's remaining tropical glaciers, thus making it important to understand how these glaciers will respond to future changes in climate. In this study, we use global climate models to calculate the freezing level height (FLH) through time (1850–2100) at the location of four monitored glaciers in the tropical Andes region of Ecuador, Peru, and Bolivia. Using the FLH, we can estimate changes in the equilibrium-line altitude at each glacier, which describes the change in the mass balance of the glacier through time. This study found that each of the four glaciers will continue to shrink rapidly, with lower elevation glaciers reaching a point of no return by the year 2100.

Key Points:

- A close correlation exists in the tropical Andes between freezing level height and glacier equilibrium-line altitudes
- This relationship can be exploited to constrain future equilibrium-line altitudes according to emission scenario and models' climate sensitivity
- Tropical Andean glaciers will continue to retreat, with some projected to lose their accumulation zone before the end of the 21st century

Correspondence to:
M. Vuille,
mvuille@albany.edu

Citation:
Turner, S. A., Vuille, M., & Rabatel, A. (2025). Constraining future projections of freezing level height and equilibrium-line altitudes in the tropical Andes based on CMIP6. *Journal of Geophysical Research: Atmospheres*, *130*, e2024JD042963. https://doi.org/10.1029/2024JD042963

Received 18 NOV 2024
Accepted 20 MAY 2025

Author Contributions:
Conceptualization: Mathias Vuille
Formal analysis: Shelby A. Turner
Funding acquisition: Mathias Vuille
Investigation: Shelby A. Turner
Methodology: Mathias Vuille
Project administration: Mathias Vuille
Resources: Antoine Rabatel
Software: Shelby A. Turner
Supervision: Mathias Vuille, Antoine Rabatel
Validation: Antoine Rabatel
Visualization: Shelby A. Turner
Writing – original draft: Shelby A. Turner, Mathias Vuille
Writing – review & editing: Mathias Vuille, Antoine Rabatel

1. Introduction

The tropical Andes mountains (~5°N–20°S) contain more than 99% of the remaining tropical glaciers (Kaser, 1999). These Andean glaciers provide important socioeconomic and environmental services and their rapid retreat thus poses a significant challenge for adaptation to changing hydrological conditions downstream for both natural and human systems (Bury et al., 2011; Carey et al., 2014; Drenkhan et al., 2015; Mark et al., 2017; Motschmann et al., 2022). As the glaciers in this region act as a hydrologic buffer, they contribute to maintaining a relatively constant river discharge downstream during the region's dry season which is critical for use in agriculture, mining, hydropower, and human consumption (Kaser et al., 2010; Mark, 2007; Saberi et al., 2019; Soruco et al., 2015; Vuille et al., 2018). However, it has been shown that, in many watersheds, the critical point of peak water has already passed and that the dry season river discharge is already decreasing (Baraer et al., 2012; Caro et al., 2024; LaFreniere & Mark, 2016). Even though glaciers are not the only water buffer, and in many regions may be supplemented or replaced by other storage systems, such as water reservoirs, wetlands (paramos), or groundwater extraction (e.g., Drenkhan et al., 2023; Somers et al., 2019), understanding how these glaciers will

respond to future changes in climate and where glaciers may disappear completely, is relevant for informing future adaptation strategies. Historically, such assessments have been challenging, as the rate of warming is amplified at higher elevations due to elevation-dependent feedbacks, which are seen in mountain regions across the globe (Pepin et al., 2015, 2022; Rangwala & Miller, 2012), including the Andes (Chimborazo & Vuille, 2021; Chimborazo et al., 2022; Urrutia & Vuille, 2009; Vuille & Bradley, 2000; Vuille et al., 2015). As global climate models (GCM's) struggle to accurately resolve the complex Andean topography, and therefore produce inaccurate mountain-top surface temperatures (Yarleque et al., 2018), relying on free-tropospheric temperature trends in GCM's tends to provide better insight into how tropical glaciers are affected by continued warming in the tropical Andes (Bradley et al., 2006, 2009; Schauwecker et al., 2014, 2017).

Recent studies have shown that Andean glaciers are among the fastest shrinking glaciers globally (e.g., Hugonnet et al., 2021; Gorin et al., 2024; The Glambie Team, 2025). Due to this rapid retreat, snow and ice melt in this region contributes up to 50% of total runoff in some basins (Caro et al., 2024). Glacier mass change estimates have previously been documented using different strategies, including extrapolation of field measurements, geodetic estimates derived from digital elevation models, low-resolution remote sensing methods which do not resolve individual glaciers, and using both global and regional climate models (Braun et al., 2019; Carrivick et al., 2024; Dussaillant et al., 2019; Fernandez & Mark, 2016; Rabatel et al., 2013; Seehaus et al., 2019, 2020; Taylor et al., 2022; Vuille, Francou, et al., 2008). Dussaillant et al. (2019) found that glacier mass balances in the tropical Andes were overwhelmingly negative from 2001 to 2017, with rapid thinning of small tropical glaciers. Indeed, most studies suggest that many tropical Andean glaciers are out of balance with the current climate and bound to continue in a state of rapid decline.

Several studies have documented a close relationship between the free troposphere 0°C isotherm (freezing level height, FLH) and the ELA of tropical glaciers (Schauwecker et al., 2014, 2017; Vuille et al., 2018; Yarleque et al., 2018). The glacier mass balance in the tropical Andes is very sensitive to increases in FLH as this determines the rain-snow line which in turn affects the albedo and the energy balance of the ablation zone (Rabatel et al., 2012, 2013; Schauwecker et al., 2017). Several studies have thus analyzed changes in the FLH in the tropical Andes using various reanalysis data sets, including ERA-Interim, ERA5, and NCEP/NCAR (Bradley et al., 2009; Rabatel et al., 2013; Schauwecker et al., 2014, 2017; Vuille et al., 2018; Yarleque et al., 2018). Bradley et al. (2009) further employed high-elevation in-situ data at Quelccaya Ice Cap (5760 m a.s.l.) to validate the FLH changes derived from multiple reanalysis data sets for the period from 1975 to 2009. They found a robust relationship, suggesting that reanalysis data sets can provide accurate assessments of free-tropospheric and near-surface temperature changes in this region that can be used to calculate FLH on monthly and annual timescales.

Since reanalysis data sets can only give insight into historical FLH changes, studies focused on future projections of FLH changes in the tropical Andes have relied on CMIP models. By using reanalysis data as the observational baseline, model simulations can be bias-corrected over the historical period, thus allowing to better constrain model projections for the end of the 21st century. Studies such as Bradley et al. (2006, 2009), Schauwecker et al. (2014, 2017), Vuille et al. (2018), and Yarleque et al. (2018) have all used previous generations of CMIP simulations to investigate projected changes in FLH over the tropical Andes throughout the 21st century. However, such assessments have generally relied on just a handful of models, and to our knowledge, no studies have taken advantage of the improvements in global climate modeling since CMIP3 and CMIP5.

However, a number of CMIP6 models are characterized by a rather high climate sensitivity compared with previous CMIP generations and climate sensitivity estimates derived from other sources, such as paleoclimatic evidence, theory, or modern observations (Smith et al., 2021). CMIP6 models include different and more sophisticated feedback processes, as well as a larger variety of physical processes when compared with earlier model generations (Hausfather et al., 2022; Meehl et al., 2020). One or multiple of these feedbacks are at the source of the "hot model" problem, resulting in excess warming in the tropics (Voosen, 2022). Indeed, in the CMIP5 generation, the highest equilibrium climate sensitivity (ECS) across all models was 4.7°C. Over one quarter of CMIP6 models have an ECS of at least 4.7°C, with around one-fifth having an ECS of 5°C or higher (Hausfather et al., 2022). Many studies have also found that these high ECS models poorly reproduce historical temperatures; specifically, often showing little warming over the twentieth century with a sharp increase in temperatures in the past few decades (Hausfather et al., 2022). The Intergovernmental Panel on Climate Change (IPCC) in its Sixth Assessment Report (AR6) has approached this problem by focusing on specific warming

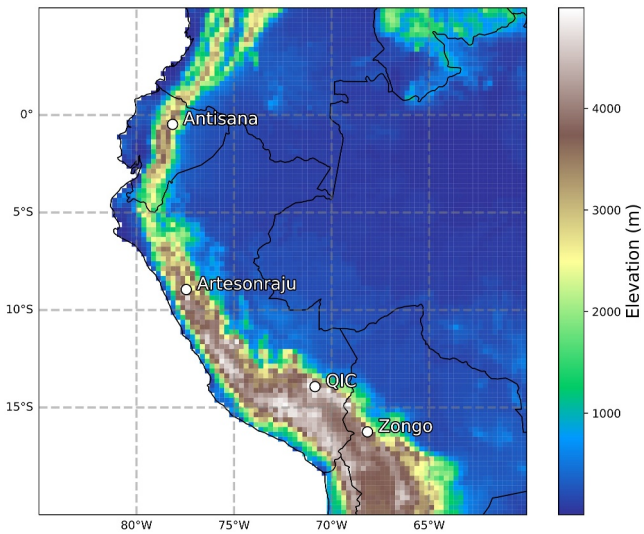

Figure 1. Topographic map outlining the spatial area of interest (5°N–20°S and 85°W–60°W), as well as the four locations of interest. Topography obtained from Global Land Data Assimilation System (GLDAS) elevation.

targets as well as exclusion of models which are known to be too hot (Hausfather et al., 2022). Studies which take these "hot models" into consideration are likely to project temperatures which become too warm too quickly.

Here, we aim to provide a better constrained estimate of future changes in FLH and glacier ELA at four tropical Andean glaciers with a long history of on-site monitoring. Using a large CMIP6 data set, we first compare the historical model runs to reanalysis data. The individual historical model simulations are based on fully coupled models and thus all contain different realizations of internal variability, affecting their phasing of interannual and decadal-scale variability. Our comparison is thus only focused on model performance in terms of the models being able to reproduce the long-term mean and standard deviation of FLH at our study sites, but not their phasing or historical trends. Relying on updated quantitative FLH-ELA relationships at all four sites, we then use the bias-corrected FLH in CMIP6 models to project future changes in the ELA under future emissions scenarios SSP2-4.5 and SSP5-8.5 using both a multi-model mean as well as estimates that exclude models that fall outside the ECS likely range. While the ECS is calculated at the global scale, this selection is nonetheless justified. As we show in this paper, models with a higher ECS also produce a stronger warming (a stronger FLH increase) over the Andes. In addition, we also assess the results when only considering those models which perform best over the historical period. Finally, these estimates are being compared with earlier ELA projections published for these same sites in Vuille et al. (2018) and Yarleque et al. (2018).

Section 2 presents the data and methods used in this study. Section 3 presents both FLH and ELA estimates for the historical period and future projections as seen in reanalysis data and models, respectively, while Section 4 discusses how these results compare to previous studies. We end with a brief summary and outlook on future work in Section 5.

2. Data and Methods

2.1. Glacier Locations and Glacier ELA Data

Here, we focus on four glaciers in the tropical Andes: glacier 15-alpha on Antisana volcano in Ecuador, glacier Artesonraju in the Cordillera Blanca in Peru, the Quelccaya Ice Cap in the Cordillera Vilcanota, Peru, and Zongo Glacier in the Cordillera Real, Bolivia (Figure 1 and Table 1). Thanks to their location extending up to high altitude summits (>5,680 m), all these glaciers still have a permanent accumulation area. The glacier surface area ranges between 0.3 km^2 for Antisana 15-alpha Glacier to more than 40 km^2 for Quelccaya. Antisana 15-alpha Glacier extends over the Antisana volcano which has not shown any sign of activity over the last four centuries (Basantes-Serrano et al., 2016). The studied glaciers are all free of debris-cover, except for the edges along the lowermost reaches of the tongue of the Artesonraju Glacier; hence, the impact on the surface mass balance is very limited. Antisana 15-alpha Glacier belongs to the inner tropics, where precipitation can occur year-round and the ablation rates on the lower tongue are almost constant year-round, reaching approximately 250 mm w.e./month. The other glaciers belong to the outer tropics where the seasonality of precipitation is well marked,

Table 1
Locations and Length of Equilibrium-Line Altitude Measurements on Glaciers Analyzed in This Study

Glacier	Mountain range	Latitude (°)	Longitude (°)	Max altitude (m)	Time period
Antisana 15 Glacier	Antisana	−0.48	−78.15	5,760	1995–2012
Artesonraju Glacier	Cordillera Blanca	−8.95	−77.45	5,979	2000–2009
Quelccaya Ice Cap	Cordillera Vilcanota	−13.93	−70.85	5,680	1992–2017
Zongo Glacier	Cordillera Real	−16.25	−68.16	6,000	1991–2014

resulting in a more pronounced seasonality in accumulation and ablation processes at the glacier surface, even if ablation can be encountered year-round at the lowermost elevations of the glacier. These locations have been chosen due to the long-term monitoring carried out at these sites (e.g., Al-Yaari et al., 2023; Autin et al., 2022; Basantes-Serrano et al., 2016, 2022; Favier et al., 2004; Francou et al., 2004; Gualco et al., 2022; Hurley et al., 2015; Rabatel et al., 2012, 2013; Reveillet et al., 2015; Sicart et al., 2005, 2011, 2014; Vuille, Kaser, & Juen, 2008; Wagnon et al., 2001) allowing for a long-term assessment of ELA and glacier mass balance changes at each site. Furthermore, earlier research based on CMIP5 models focused on these same locations, allowing for a comparison across CMIP model generations and a temporal extension of earlier results (Vuille et al., 2018; Yarleque et al., 2018). Here, we use the annual mean ELA values reported in Vuille et al. (2018), and Yarleque et al. (2018), spanning varying time periods between 1991 and 2017, depending on the glacier considered (see Table 1). The annual mean was calculated using the hydrologic year, which is January to December in Ecuador and September through August in Peru and Bolivia. These ELA time series were further complemented with more recent unpublished estimates provided by the French GLACIOCLIM program (https://www.ige-grenoble.fr/GLACIOCLIM).

It is important to note that the ELA represents an estimated value based on spatial interpolation of individual point-based measurements of the mass balance on the glacier. Most mass balance measurements are taken in the ablation zone at lower elevations of the glacier using an ablation stake network, while measurements in the accumulation zone at the upper reaches of the glacier using a network of snow pits are less frequent, leading to some uncertainty in ELA measurements. At Quelccaya, instead of actual ELA measurements, end of the dry season snowlines were used as approximations of the ELA. The validity of this assumption is discussed and demonstrated in detail in Rabatel et al. (2012) and Yarleque et al. (2018). In general, the uncertainty in determining the ELA, quantified from in situ measurements, depends mostly on the number of available data points. The ELA is computed by linearly regressing the surface mass balance measurements against the altitude of these point-measurements. The ELA uncertainty is then calculated based on the standard error of this linear regression. It varies between ±10 m to ±55 m, depending on year and location, with an average of ±27 m. On the Quelccaya ice cap, the ELA is quantified using the dry season snowline. Here, the uncertainty depends on several factors, discussed in detail in Yarleque et al. (2018), and ranges between 70 and 110 m, with an average of 90 m.

A spatial analysis of temporal FLH trends was also completed over the tropical Andes region, as defined by 5°N–20°S latitude and 85°W–60°W longitude and shown in Figure 1.

2.2. CMIP6 Model Data

Earlier studies used only a small subset of CMIP5 models (Vuille et al., 2018; Yarleque et al., 2018) while here we rely on a much larger set of CMIP6 models to better constrain future FLH and ELA projections. A study completed by Almazroui et al. (2021) used 37 models from CMIP6 and investigated their performance over South America. It was found that these models successfully captured the main climate characteristics of the region. Here, we make use of 35 of the 37 models analyzed in Almazroui et al. (2021) (see Table 2). Two models included in Almazroui et al. (2021) were omitted here as they were not available in the Earth System Grid Federation (ESGF) model repository. In a portion of the results section, these models are differentiated numerically based on their model number from Almazroui et al. (2021), which is replicated in Table 2. Monthly model output was obtained for each of the variables of interest, air temperature (ta), and geopotential height (z) at three pressure levels (600 hPa, 500 hPa, and 400 hPa). These variables were resampled for each model onto a 1° lat. × 1° lon. grid across the entire globe using the Climate Data Operators (CDO) package command "remapnn," which uses nearest neighbor remapping, to ensure all grid points matched in latitude and longitude across models for a more precise comparison. Finally, for the spatial analysis, data for the region defined above, were selected using the CDO command "sellonlatbox," as data from the rest of the globe were discarded.

Three CMIP6 experiments were used in this study: historical, SSP2-4.5, and SSP5-8.5. The historical experiment is primarily for model validation in comparison to observational data and covers the time period 1850–2014. It is forced by both natural forcings such as volcanic aerosols and solar variability, as well as anthropogenic forcings such as CO_2 concentration, aerosols, and land use changes (Eyring et al., 2016). However, coupled models also contain unforced variability which can cause differences in the phasing of internal variability between observations and historical simulations.

Table 2
Description of Each Model Used in This Project

Number	Model	Institution country	Variant label	ECS (°C)
1	ACCESS-CM2	Australia	r1i1p1f1	4.72
2	ACCESS-ESM1-5	Australia	r1i1p1f1	3.87
3	AWI-CM-1–1-MR	Germany	r1i1p1f1	3.16
4	BCC-CSM2-MR	China	r1i1p1f1	3.04
5	CAMS-CSM1-0	China	r1i1p1f1	2.29
6	CanESM5-CanOE	Canada	r1i1p2f1	5.62
7	CanESM5	Canada	r1i1p1f1	5.62
8	CESM2	USA	r4i1p1f1	5.16
9	CESM2-WACCM	USA	r1i1p1f1	4.75
10	CMCC-CM2-SR5	Italy	r1i1p1f1	3.52
11	CMCC-ESM2	Italy	r1i1p1f1	3.57
12	CNRM-CM6-1	France	r1i1p1f2	4.83
13	CNRM-CM6-1-HR	France	r1i1p1f2	4.28
14	CNRM-ESM2-1	France	r1i1p1f2	4.76
15	EC-Earth3	Europe	r1i1p1f1	4.31
16	EC-Earth3-Veg-LR	Europe	r1i1p1f1	4.31
17	EC-Earth3-Veg	Europe	r2i1p1f1	4.31
18	FGOALS-f3-L	China	r1i1p1f1	3
19	FGOALS-g3	China	r1i1p1f1	2.88
20	FIO-ESM-2-0	China	r1i1p1f1	–
21	GFDL-ESM4	USA	r1i1p1f1	2.6
22	GISS-E2-1-G	USA	r1i1p1f2	2.72
24	IITM-ESM	India	r1i1p1f1	–
25	INM-CM4-8	Russia	r1i1p1f1	1.83
26	INM-CM5-0	Russia	r1i1p1f1	1.92
28	MCM-UA-1-0	USA	r1i1p1f2	3.65
29	MIROC6	Japan	r1i1p1f1	2.61
30	MIROC-ES2L	Japan	r1i1p1f2	2.68
31	MPI-ESM1-2-HR	Germany	r1i1p1f1	2.98
32	MPI-ESM1-2-LR	Germany	r1i1p1f1	3
33	MRI-ESM2-0	Japan	r1i1p1f1	3.15
34	NESM3	China	r1i1p1f1	4.72
35	NorESM2-LM	Norway	r1i1p1f1	2.54
36	NorESM2-MM	Norway	r1i1p1f1	2.5
37	TaiESM1	Taiwan	r1i1p1f1	4.31

Note. The ECS for each model was obtained from IPCC AR6 Chapter 7 supplementary material (Smith et al., 2021). Note that 35 models were used in total as models # 23 and 27 were not available in the ESGF repository.

There are a total of nine shared socio-economic pathways (SSP) scenarios for the 21st century and beyond. Only two were used in this project to ideally bracket the most plausible range of ELA changes between 2005 and the year 2100. SSP2-4.5 is a part of the second tier of SSP scenarios which includes "middle of the road" scenarios, with an increase in radiative forcing of 4.5 W/m^2, roughly corresponding to RCP-4.5 in CMIP5 (Meinshausen et al., 2020). SSP5-8.5 represents the upper end of the SSP scenarios, with the world being heavily reliant on fossil fuels throughout the 21st century, and radiative forcing increasing to 8.5 W/m^2 (Meinshausen et al., 2020). Both scenarios were included in the IPCC AR6 as "high-priority scenarios."

2.3. Reanalysis Data

Data from the fifth generation of the European Center for Medium-Range Weather Forecasts (ECMWF) atmospheric reanalysis (ERA5, Hersbach et al., 2023) were used for analysis based on their superior performance over the tropical Andes as shown in Schauwecker et al. (2017) and Birkel et al. (2022). Monthly-averaged ERA5 geopotential and temperature data from 1959 to 2015 for the 400 hPa, 500 hPa, and 600 hPa pressure levels were obtained from the ECMWF Climate Data Store (CDS). Geopotential height was then calculated by dividing the geopotential by Earth's gravitational acceleration (9.80665 m/s). The ERA5 data were resampled to a 1° lat. × 1° lon. grid to match the resolution of the CMIP6 models for analysis, and the data over the domain of analysis were selected using the same method as discussed in Section 2.2.

2.4. Determination of FLH

The FLH was calculated at each grid point and for each month by linearly extrapolating temperature between the two pressure levels bracketing the 0°C isotherm using the xarray package in python, as well as by defining two functions to complete the algebraic steps. The first function was defined as "grad." This function calculated the linear temperature lapse rate between the two pressure levels. The next function was defined as "height." This function used the lapse rate and the slope of the geopotential height between the two encompassing pressure levels to determine the height of the 0°C isotherm. By doing this, four different data sets were created which, when combined, created a 3-dimensional data set at 1° spatial resolution, containing the FLH at every latitude and longitude through time. Finally, the monthly FLH values were converted to yearly averages. This analysis was applied separately to each model/scenario and at each of the four glacier locations.

Both temporal and spatial analyses were completed for ERA5 and all CMIP6 models. Temporal analyses were completed only for the four mountain regions discussed above, by calculating the FLH at the grid box encompassing the glacier of interest, and the eight surrounding grid boxes. The nine FLH values were then averaged to obtain the final FLH at that time.

2.5. Trend Calculation and Significance Testing

The trend of the FLH was calculated at each grid box across the domain to allow for a spatial analysis and a comparison between models and reanalysis products over the historical period. The trend was calculated for the period of overlap between CMIP6 models and ERA 5, 1959–2015. For the future projections, the trends were calculated for the period 2015–2100 for both scenarios. To calculate the trend, a pandas data frame was created and using the stats package from scipy, the slope of the FLH in this array was calculated using ordinary least squares regression. For the historical scenario,

this was completed for each of the 35 models for the 1850–2015 and 1959–2015 time periods, as well as for ERA5 for the 1959–2015 period. This analysis was also completed for the two future scenarios for each of the 35 models for the 2015–2100 time period.

An *F*-test was used to calculate the significance of the FLH trend by finding the p-value of the trend at each grid point for the historical simulations and the two future projections for all CMIP6 models and for ERA5. The *p*-value describes the probability that the slope is not significantly different from zero. Unless noted otherwise, a *p*-value of less than 0.05 is considered a significant trend.

2.6. Bias Correction

Here, we consider the ERA5 reanalysis data to be the observational target against which the CMIP6 model data are compared. Reanalysis data, unlike CMIP6, is based on assimilated data from satellites, radiosondes, and surface observations. Previous studies such as Birkel et al. (2022) have shown ERA5 to be more accurate than other reanalysis products in this region, leading us to rely on ERA5.

Each CMIP6 model's bias, when compared with ERA5 was calculated using the delta change method for bias correction (Ho et al., 2012). The mean value of the FLH was calculated from 1959 to 2015 (ERA5 time period) for each model as well as for ERA5 at each of the four glacier locations. To minimize individual grid box uncertainties, these values were based on the FLH averaged over the closest grid box and the eight surrounding grid cells. These values were used to find the average FLH difference between the model and ERA5, resulting in a bias estimate (in m) for each of the 35 models over the four glacier locations of interest. The appropriate bias-correction was then applied to the calculated projected FLH to obtain the bias-corrected FLH for each location and time.

The interannual variability of the FLH simulated by CMIP6 historical runs was also compared with the FLH interannual variability in ERA5 at each glacier site. This was achieved by calculating the standard deviation of the FLH in ERA5 and each of the CMIP6 models during the period of overlap (1959–2015). The standard deviation of the FLH time series was calculated using the NumPy package in python. This comparison was used together with the bias estimate to rank CMIP6 models and select models that perform the best over the historical period for one set of future FLH change analyses.

2.7. ELA Calculation

As shown in Vuille et al. (2018) and Yarleque et al. (2018), there is a significant linear relationship between ELA and FLH in the tropical Andes. At each glacier location, a linear regression was thus performed to determine the linear dependence of the ELA on the FLH as determined by ERA5. This linear relationship between FLH and ELA, determined at each glacier for the time period specified in Table 1, was then applied to the bias-corrected CMIP6 model projections to obtain estimated future ELA changes. However, this method includes several assumptions and simplifications. As will be discussed in Sections 3 and 4, there are many additional factors that impact the ELA, such as snow accumulation, elevation feedbacks, and ice-albedo feedbacks. However, the close correlation between ELA and FLH suggests that the role played by these other factors is either relatively minor compared with the dominant role played by variations in the FLH, or that these aspects are incorporated in the observed empirical relationship. As discussed in more detail in Vuille et al. (2018), these assumptions result in future ELA estimates that likely err on the conservative (low) side of potential future outcomes.

3. Results

3.1. Historical Comparisons

The FLH values found in ERA5 at the four investigated glacier sites agree in range with previous analyses such as Rabatel et al. (2013), Schauwecker et al. (2017), Vuille et al. (2018), and Yarleque et al. (2018). The temporal analysis for the four glacier locations shown in Figure 2 suggests that the difference in the mean FLH between ERA5 and the CMIP6 multi-model mean becomes larger, the farther away from the equator the glacier is located. At Antisana 15, being the glacier located the closest to the equator, the differences in the mean FLH between the two data sets are minor. The FLH of ERA5 falls well within one standard deviation of the CMIP6 multi-model mean for both Antisana Glacier and Artesonraju Glacier. However, at the Quelccaya ice cap and on Zongo

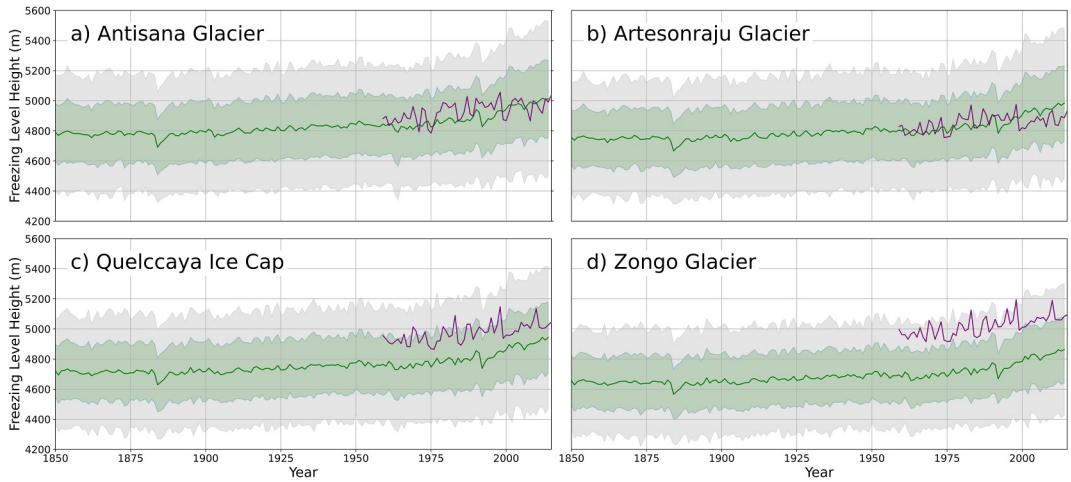

Figure 2. Annual mean freezing level height (FLH) in meters during the historical period (1850–2015), with the CMIP6 multi-model mean in green, ±1σ shaded in green, ±2σ shaded in gray, and ERA5 in purple for the four glaciers and ice caps of interest: (a) Antisana 15 Glacier, (b) Artesonraju Glacier, (c) Quelccaya Ice Cap, and (d) Zongo Glacier.

Glacier, the CMIP6 multi-model mean FLH begins to stray from the ERA5 FLH values. At Zongo Glacier, the ERA5 FLH values are nearly two standard deviations higher than the CMIP6 multi model mean.

The typical FLH at each mountain region varies based primarily on each location's distance from the equator. Antisana Glacier has the highest FLH throughout the time period, with CMIP6 historical FLH values starting at around 4,800 m in 1850 and ending around 5,000 m in 2015. The farther away the mountain range is located from the equator, the lower the FLH, with the lowest FLH in 1850 being about 4,600 m on Zongo Glacier, with FLH increasing by ∼200 m to 4,800 m by 2015. The majority of this increase occurs at the end of the time period, between 1975 and 2015.

The CMIP6 multi-model mean FLH remains nearly constant for all four mountain regions until around 1975, when it begins to increase. This is consistent with the enhanced warming observed in the region over recent decades (e.g., Vuille et al., 2015). However, this increase is less dramatic in the ERA5, when compared with CMIP6, as shown in the spatial trend analysis (Figure 3). The FLH change across all CMIP6 model may not follow a normal distribution given that there may be some "hot" models that result in a long tail at the upper end of the distribution. We thus also plot the median trend in Figure 3c. Finally, we also consider results based on a subset of models, analyzing only CMIP6 models with an equilibrium climate sensitivity that falls within the Intergovernmental Panel on Climate Change "likely" range (Figure 3d). In general, the results do not deviate significantly from one another, regardless of the criterion used for the model selection, or whether the mean or the median are considered. The trend in the FLH is slightly larger in the ECS-constrained case, likely because this model subset also excludes a few "cold" models.

There exist also large differences in the spatial pattern of the FLH trends between ERA5 and CMIP6. In the CMIP6 data, the weakest trends occur in the southernmost part of the domain while ERA5 data show the opposite effect, with the strongest trends located over the southernmost part of the domain. These model results are consistent with Schauwecker et al. (2017) who performed a similar analysis based on a CMIP5 multi-model mean and who also found the same spatial pattern as identified here for CMIP6.

Comparing trends between CMIP6 and reanalysis data sets needs to consider that a multi-model CMIP6 average will cancel out internal variability and only reflects the anthropogenically forced trend, while the individual reanalysis products also contain internal variability, which can modulate trends, especially on shorter timescales and over the eastern Pacific region. Nonetheless, these results suggest that CMIP6 models contain a significant bias in their FLH estimates; hence, corrections to the CMIP6 FLH values are necessary to better constrain projections of FLH and ELA. The removal of identified "hot" models with a high ECS could also potentially correct the strong trend of CMIP6 models near the end of the twentieth century. Applying both corrections to future scenarios should result in better constrained estimates of future changes in FLH and ELA.

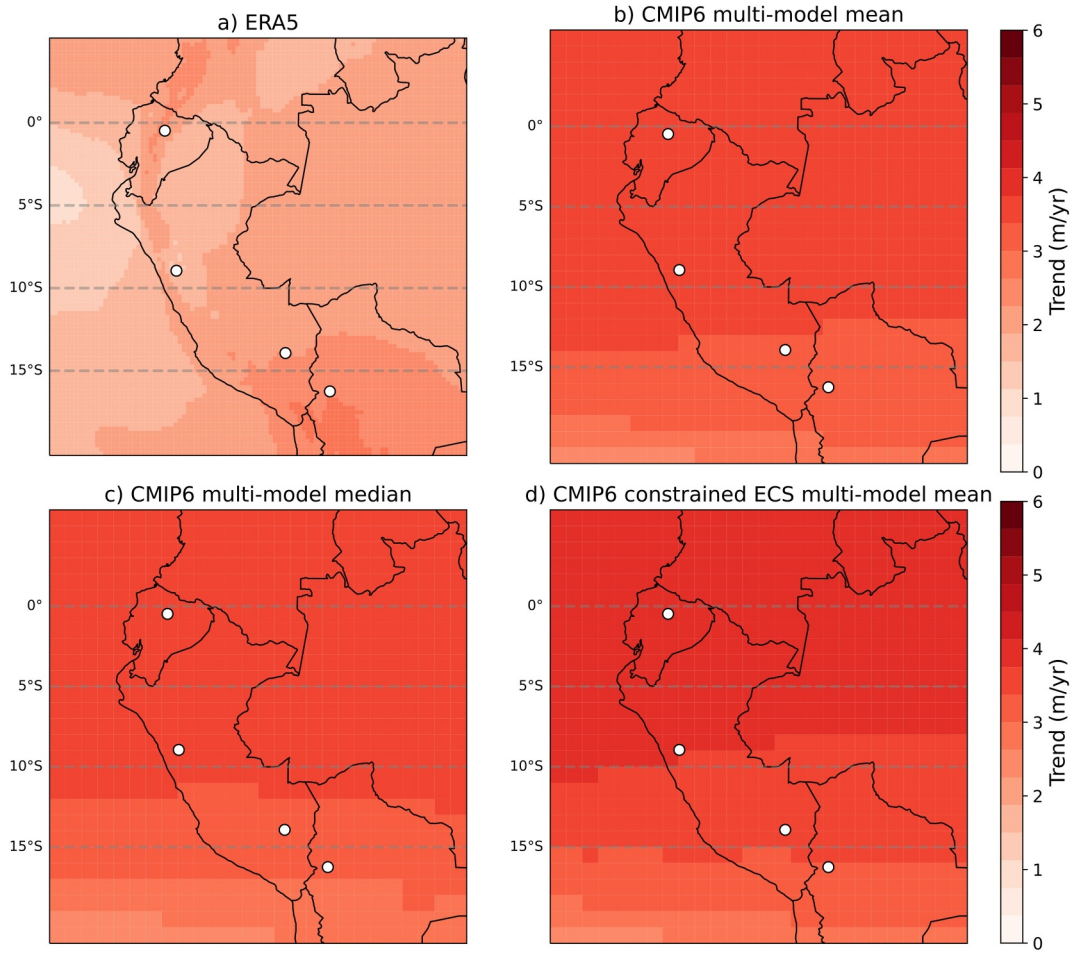

Figure 3. (a) Mean freezing level height (FLH) trend for ERA5, (b) as in panel (a) but for CMIP6 multi-model mean, (c) as in panel (b) except based on median FLH, (d) as in panel (b) except for subset of models with equilibrium climate sensitivity within Intergovernmental Panel on Climate Change "likely" range. All analyses are for period 1959–2015. Trends (p-value <0.05) are significant everywhere. White dots indicate locations of the four glaciers and ice caps investigated.

3.2. Bias and Standard Deviation Comparisons

The CMIP6 FLH bias (difference in the mean FLH when compared with the reanalysis data set) and standard deviation difference was calculated for each of the 35 models for the four mountain regions. Figure 4 shows the bias and standard deviation of each model when compared with ERA5 at each location quantified for the period 1959–2015.

Overall CMIP6 models perform quite well near the equator, with mean FLH values being very similar to ERA5. However, in the outer tropics (Quelccaya ice cap and especially on Zongo glacier), the models place the FLH at an elevation that is significantly too low, revealing that the models tend to be too cold in this region. The majority of CMIP6 models simulate a higher FLH standard deviation than ERA5, with only between two and five models (depending on location) having a FLH standard deviation that is lower than in ERA5. This suggest that in general the CMIP6 models are overestimating the interannual variability of the FLH compared to ERA5. Based on this analysis, we select a subset of "best-performing" models that we use for further analysis to assess to what extent model choice affects the outcome of the results. For this subset, we choose models whose FLH bias is less than 250 m (i.e., the simulated FLH is within a range of ±250 m from the ERA5 FLH) and whose interannual variability, as expressed by the standard deviation, differs by less than 40 m from the ERA5 standard deviation. This analysis was performed separately at each of the four glacier locations and resulted in 16 "best-performing" models for Antisana, 9 for Artesonraju, 11 for Quelccaya Ice Cap, and 12 for Zongo.

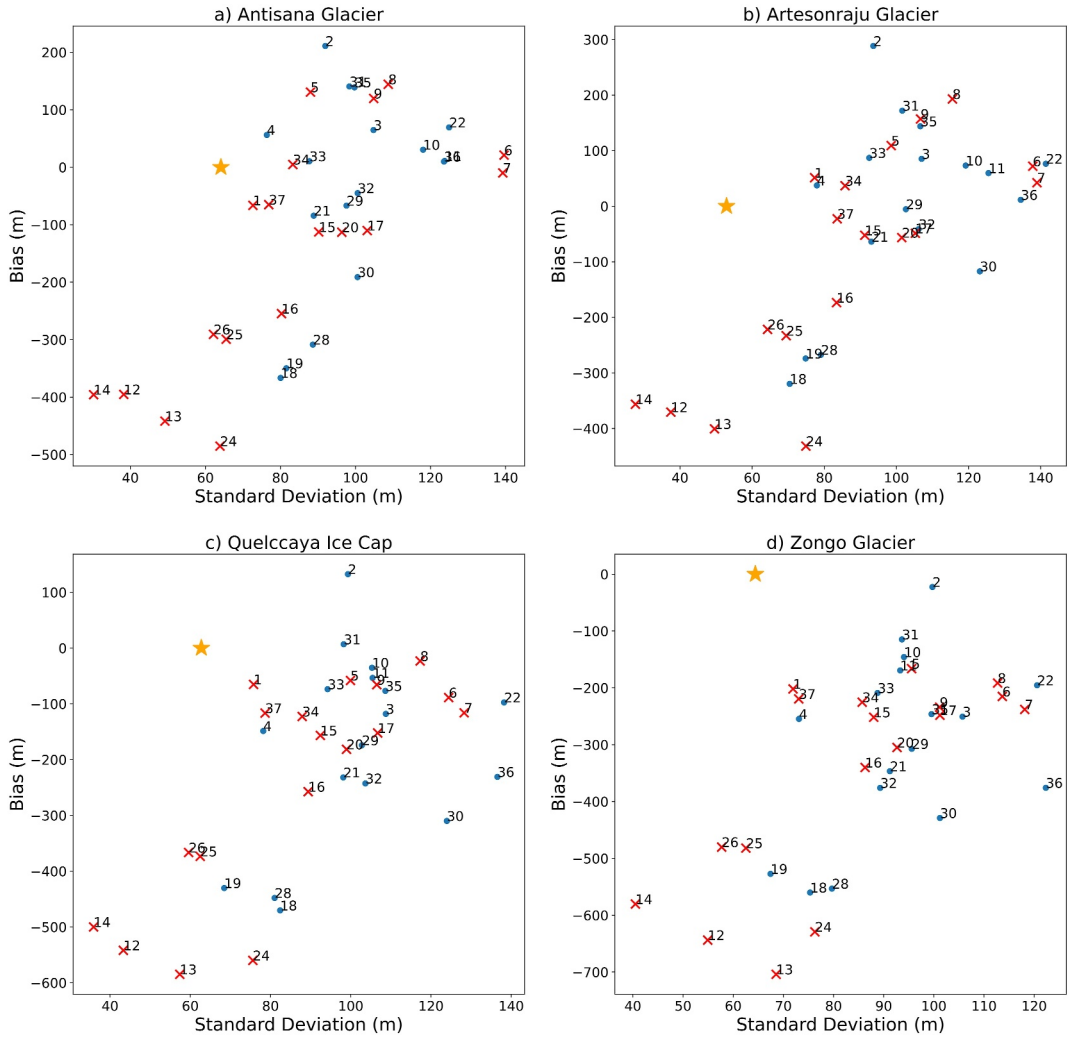

Figure 4. CMIP6 model bias and standard deviation for freezing level height (FLH) estimates when compared with ERA5 for each glacier location. ERA5 FLH is shown as yellow star; models with an equilibrium climate sensitivity inside (outside) the Intergovernmental Panel on Climate Change "likely" range are represented by a red cross (blue dot), respectively. Each model is labeled with the corresponding model number (from Table 2). Note that scale for *y*- and *x*-axes varies between panels.

3.3. Future CMIP6 FLH Projections

Similar to the analysis for the historical period shown in Figure 3, a spatial analysis of projected future FLH changes was completed for CMIP6 SSP2-4.5 and SSP5-8.5 (Figure 5). There is a large difference in the magnitude of the trend in FLH between the two scenarios. The multi-model mean trend from 2015 to 2100 for SSP2-4.5 ranges from 4.9 m/yr to 5.7 m/yr throughout the region while for SSP5-8.5 it ranges from 10.7 m/yr to 12.3 m/yr. The two scenarios agree spatially, with the largest trends occurring to the east of the Andes near 5°S. This pattern is driven by the enhanced release of latent heat during condensation resulting from intensified convection, which leads to strong warming of the mid- and upper troposphere in the tropics and subtropics, as outlined in Bradley et al. (2006). This trend of warming of the lower and mid-troposphere generally tends to decrease polewards, with the lowest warming in both scenarios occurring in the subtropics over the SE Pacific. For the investigated glacier locations this implies that Antisana and Artesonraju Glacier show a similar increase in the FLH throughout the 21st century, with the FLH trend at both locations being around 5.6 m/yr (SSP2-4.5) and 12.1 m (SSP5-8.5), respectively. Quelccaya Ice Cap and Zongo experience slightly smaller trends of around 5.4 m/yr and 5.3 m/yr (SSP2-4.5) and 11.7 m/yr and 11.5 m/yr (SSP5-8.5), respectively.

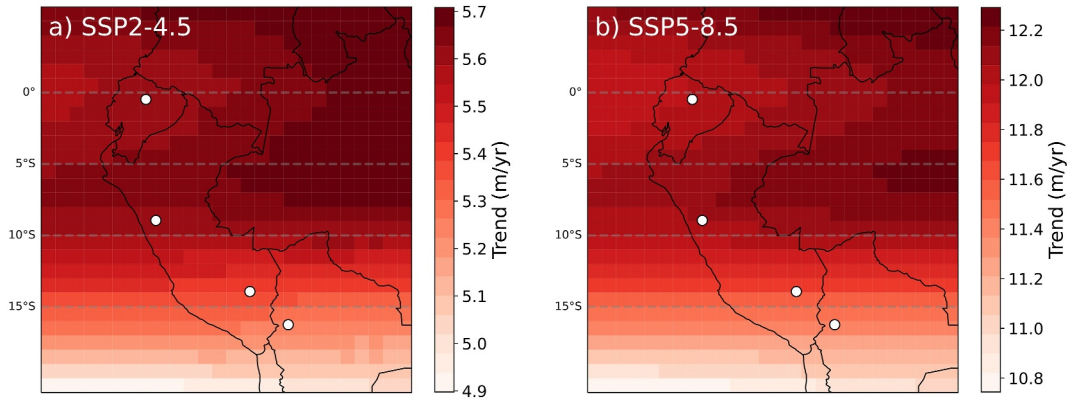

Figure 5. The change in annual mean freezing level height (FLH) (in m/yr) from 2015 to 2100 in the CMIP6 multi-model mean for the (a) SSP2-4.5 and (b) SSP5-8.5 scenario. Note that the scale is different in (a) and (b). The trend is significant everywhere ($p < 0.05$). Small white dots indicate locations of the four glaciers and ice caps investigated.

Figure 6 shows the yearly-averaged and bias-corrected FLH for each mountain region from 1850 to 2100 in SSP2-4.5 and SSP5-8.5. The bias correction leads to a significant reduction of the FLH spread across CMIP6 models and to an upward shift in mean elevation, as the model bias was mostly negative (Figure 4).

The higher emissions scenario SSP5-8.5 shows a much larger increase in FLH than the moderate emissions scenario at each location, which is expected. There is a nonlinear increase in the FLH trend throughout the 21st century in SSP5-8.5 while the rate of growth decreases in the SSP2-4.5 scenario. The variation of FLH through time is similar for each mountain region, but the magnitude does change depending on the latitudinal position.

The projected multi-model mean FLH increase from 2015 to 2100 ranges between ∼375 m (Zongo, Quelccaya) and ∼500 m (Antisana) in SSP2-4.5 and between ∼875 m (Quelccaya) and ∼1,000 m (Antisana) in SSP5-8.5. By the year 2100, this results in the multi-model mean FLH being located between ∼5400 m (Artesonraju) and ∼5,500 m (Antisana, Quelccaya, Zongo) for SSP2-4.5 and between ∼5950 m (Artesonraju) and ∼6,000 m (Antisana, Quelccaya, Zongo) in SSP5-85. As a result of this increase, in the SSP5-8.5 scenario, the FLH emerges above the maximum glacier elevation on Quelccaya ice cap sometime between the years 2052 and 2063, depending on which model subset is used to calculate the mean FLH (Table 3). In the SSP2-4.5 scenario, this emergence occurs later, between 2059 and 2075, although the FLH never emerges above the maximum glacier

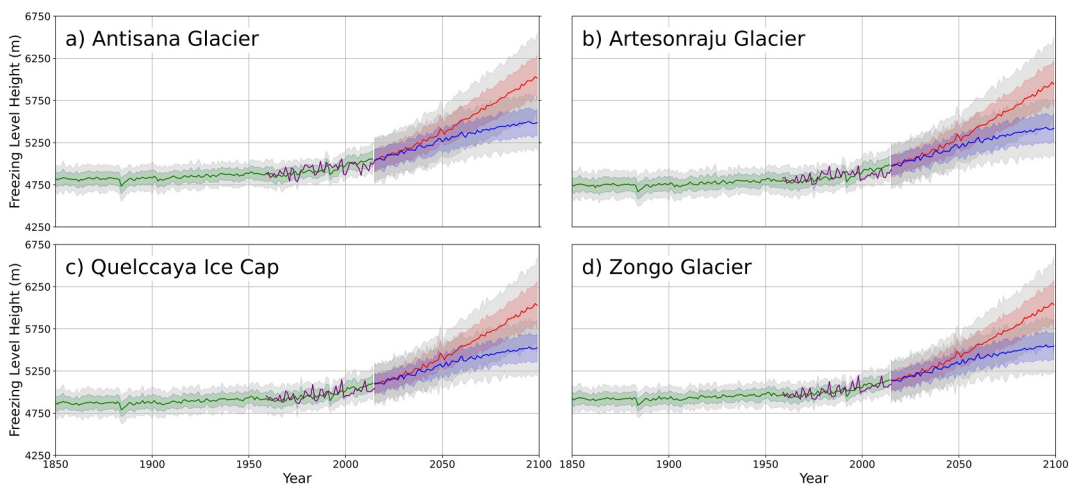

Figure 6. Bias-corrected annual mean freezing level height (FLH) for each location between 1850 and 2100 in models and reanalysis: (a) Antisana Glacier, (b) Artesonraju Glacier, (c) Quelccaya Ice Cap, and (d) Zongo Glacier. The CMIP6 historical multi-model mean is shown in green, ERA5 in purple, the SSP2-4.5 multi-model mean in blue, and SSP5-8.5 in red. The colored shading represents ±1σ from the corresponding simulation's multi-model mean, and the gray shading represents ±2σ from the multi-model mean.

Table 3
"Emergence" (the First of Five Consecutive Years) of the Freezing Level Height Above the Maximum Glacier Elevation as a Function of Emission Scenario, Glacier Location, and Model Choice

SSP2-4.5	Antisana	Artesonraju	Quelccaya	Zongo
All	–	–	–	–
Bias-Corrected	–	–	2068	–
ECS-Constrained	–	–	2075	–
Best-performing	–	–	2059	–
SSP5-8.5	**Antisana**	**Artesonraju**	**Quelccaya**	**Zongo**
All	2080	–	2063	–
Bias-Corrected	2079	–	2052	–
ECS-Constrained	2083	–	2056	–
Best-performing	2079	–	2052	–

elevation in this scenario if all models are considered. "Emergence" here refers to the first of five consecutive years with a FLH above the maximum glacier elevation. On Antisana, this emergence occurs between 2079 and 2083 in SPP5-8.5, but the FLH stay below the maximum glacier elevation in all cases under the SSP2-4.5 scenario (Table 3). The same is also true for both scenarios on Artesonraju and Zongo glaciers (Table 3).

3.4. ELA-FLH Relationships

At each location, ELA observations were used to find the linear relationship between FLH and ELA. Figure 7 shows the ordinary least-squares linear regression between FLH and ELA at each location, as well as the equations used to derive the ELA from the FLH. Both the *r*- and *p*-values for all locations reveal a close relationship between ELA and FLH, consistent with previous studies (Vuille et al., 2018; Yarleque et al., 2018). The *p*-values, which in this case indicate the significance of the correlation, are at or below 0.05 at all the locations. Artesonraju glacier (Figure 7b) shows the most sensitive ELA, with a 0.92 m rise in the ELA for every 1 m rise in FLH. Quelccaya Ice Cap (Figure 7c) resides at the other end of the spectrum as the ELA rises by only 0.56 m for each 1 m rise in FLH.

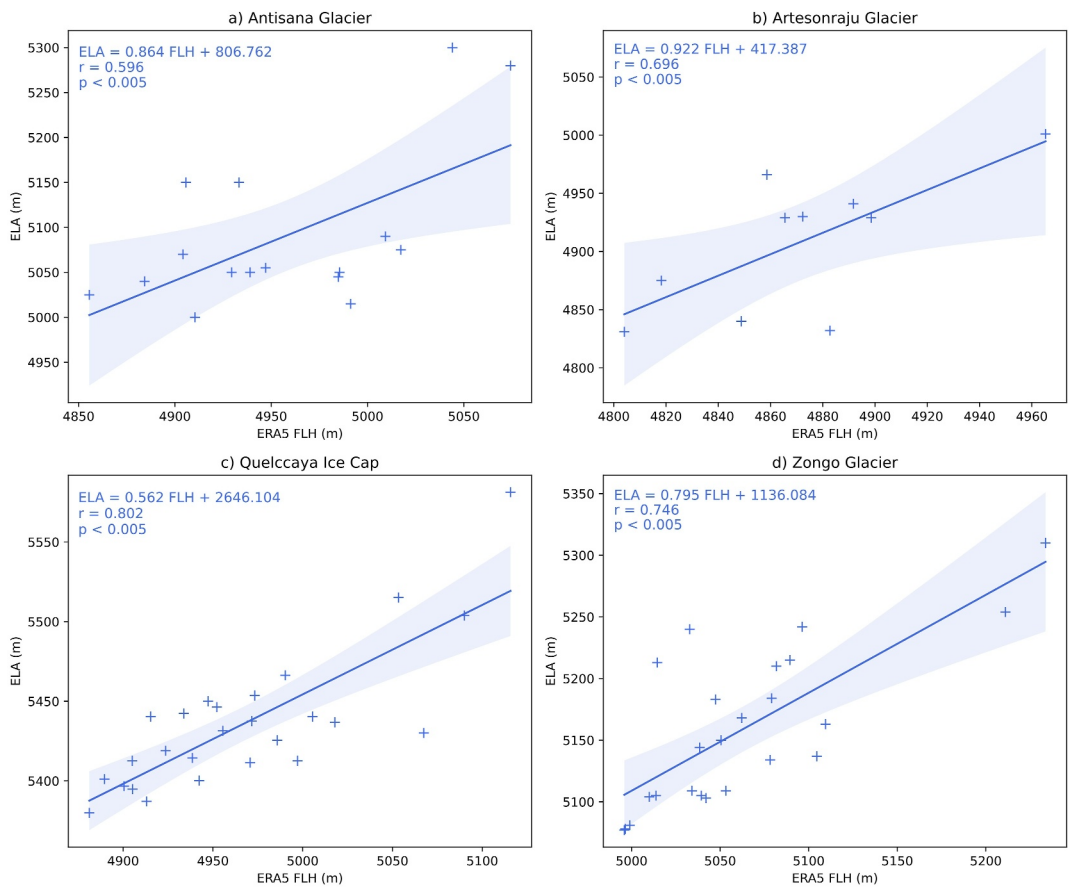

Figure 7. Scatter plots of equilibrium-line altitude (ELA) vs. bias-corrected freezing level height (FLH) for each location: (a) Antisana Glacier, (b) Artesonraju Glacier, (c) Quelccaya Ice Cap, and (d) Zongo Glacier. The ordinary least-squares linear regression is plotted with the equation, *r*-value, and *p*-value indicated. Note that scales for *y*- and *x*-axes vary between plots. The blue shading indicates the 95% confidence interval for the slope of the regression (F-test).

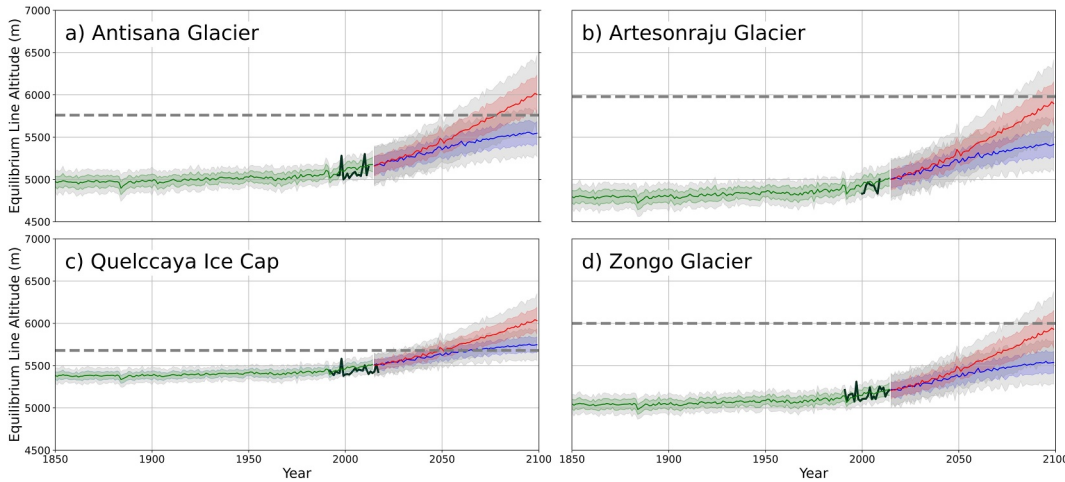

Figure 8. The annual mean estimated equilibrium-line altitude (ELA) for each location: (a) Antisana Glacier, (b) Artesonraju Glacier, (c) Quelccaya Ice Cap, and (d) Zongo Glacier. The CMIP6 historical multi-model mean is shown in green, ELA observations are plotted in black, the SSP2-4.5 multi-model mean is shown in blue, and the SSP5-8.5 scenario in red. The colored shading indicates ±1σ from the corresponding simulation's multi-model mean, and gray shading represents ±2σ from the multi-model mean. The horizontal black dashed line indicates the highest altitude of the glacier at each location.

While the correlation coefficient (r) is significant at all locations, the r-values vary in strength across the four sites. This can be attributed in part to uncertainties in the ELA measurements, which are heavily skewed toward the ablation zone, but also to the short data periods (especially at Artesonraju), and the dependence of the ELA on factors other than the FLH. At Antisana and Artesonraju glaciers in particular, the relationship is susceptible to the accuracy of a few measurements that were made during years with high FLH. Nonetheless, the F-test reveals that the slope (dependence of the ELA on FLH variations) is significantly different from zero at all four locations, as indicated by the confidence intervals of the regression slope (blue shading in Figure 7).

3.5. ELA Projections

By applying the observed ELA-FLH relationship to historical and future FLH estimates, the bias-corrected FLH values were converted to ELA estimates, resulting in estimated ELA changes from 1850 to 2100 at each glacier location, as shown in Figure 8. The dashed line in each plot signifies the highest altitude of the glacier at each location (as shown in Table 2). This allows interpreting the ELA changes from a glacier change perspective, as the mass balance of a glacier is positive only above the ELA. Hence, once the ELA moves beyond the highest reaches of the glacier, this glacier will have lost its accumulation zone and eventually disappear. The ELA results are broadly similar to the FLH results explained in Section 3.3, in the sense that the higher emissions scenario is showing a larger model spread, as well as a significantly larger rate of increase than the intermediate emissions scenario for each location.

Figure 8 suggests that the accumulation zone of Antisana Glacier and Quelccaya Ice Cap are projected to disappear before the year 2100 under the high-emission scenario. However, only Quelccaya Ice Cap is projected to disappear by 2100 in both the high- and intermediate-emission scenario. The high-emission scenario multi-model mean ELA is projected to be around 6,000 m in 2100 at Antisana Glacier, ∼5,900 m at Artesonraju Glacier, just above 6,000 m at Quelccaya Ice Cap, and ∼5,900 m at Zongo Glacier. The intermediate emission scenario multi-model mean ELA is expected to be just over 5,500 m at Antisana Glacier, 5,400 m at Artesonraju Glacier, ∼5,700 m at Quelccaya Ice Cap, and ∼5,500 m at Zongo Glacier.

As shown in Figure 9, there is a clear linear relationship between the CMIP6 model's ECS and their projected future FLH changes (and thus, also their ELA changes). Indeed, the projected future FLH change (year 2100–year 2015) under the SSP5-8.5 scenario is more than twice as large in models with an ECS >4.5°C, when compared with models with an ECS <2.5°C.

Given the strong dependence of the future FLH on the individual models' ECS, we further constrained these ELA estimates by only considering models with an ECS that lies within the “likely” range defined by the IPCC AR6:

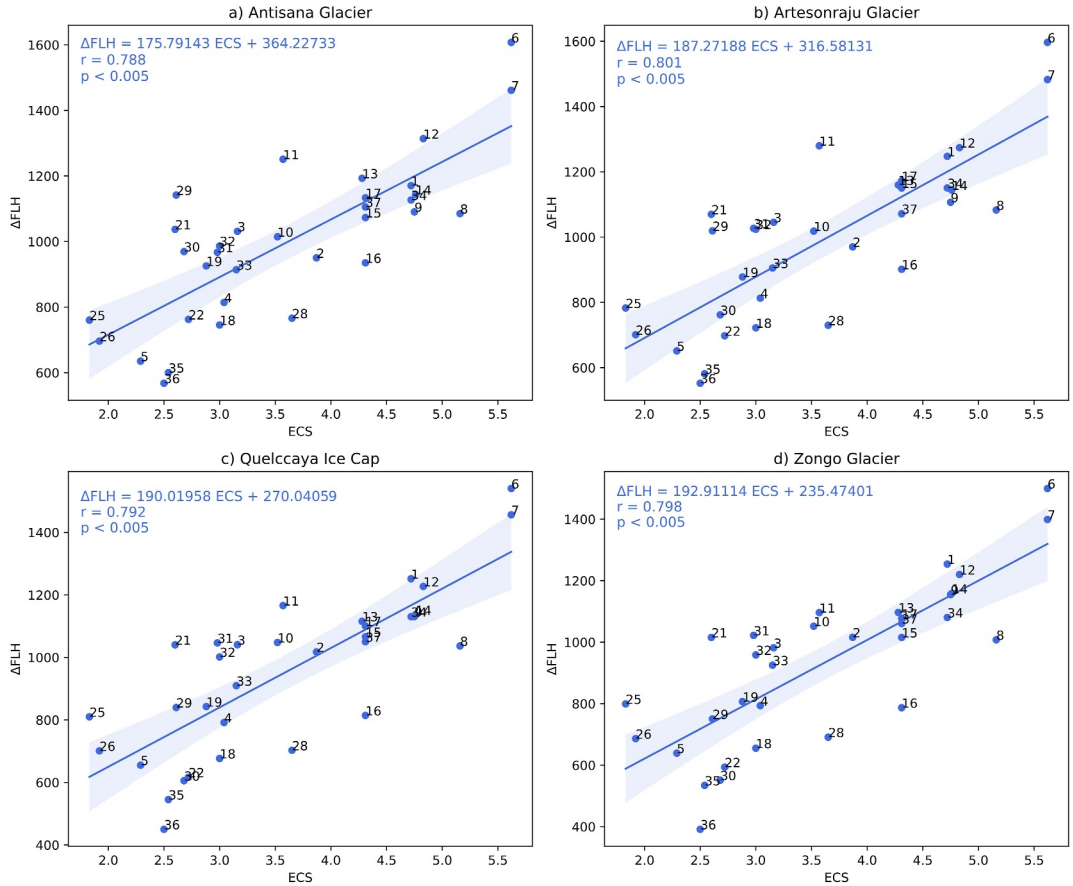

Figure 9. Relationship between equilibrium climate sensitivity (ECS, in °C) and projected future change in freezing level height (2100–2015, in m) at (a) Antisana Glacier, (b) Artesonraju Glacier, (c) Quelccaya Ice Cap, and (d) Zongo Glacier) under the SSP5-8.5 scenario for 33 CMIP6 models. Numbers next to each point refer to the corresponding model number from Table 2. Note that two of the models used did not report an ECS value, hence they were omitted in this analysis.

2.5°C–4°C. Table 2 lists the ECS of each model, with only 17 of the 35 CMIP6 models used having an ECS within the IPCC AR6 likely range, 13 of the models having an ECS above, and 3 below that range. For the remaining two models, no ECS value was indicated in Smith et al. (2021), hence these models were not included in the following analysis.

The impact of using a more constrained ECS can easily be seen when looking at Figure 10, which shows a much narrower range of model-estimated ELA. This applied constraint also decreases the projected ELA in 2100 at each location; however, it does not decrease the ELA below the maximum altitude in any location or scenario where it rose above that altitude in the full model ensemble.

Finally, we also show the results when only considering the "best-performing" models (Figure 11). Overall, the differences are minor compared with the results when including all bias-corrected models (Figure 8), suggesting that model skill over the historical period may not be as relevant of a predictor for model choice. It is further noteworthy that selecting the "best-performing" models only does not lead to a reduction in uncertainty. In fact, the model spread is significantly larger than when constraining model selection based on their ECS (Figure 10).

4. Discussion

The current FLH at the four glacier locations investigated in this study is consistent with earlier estimates by Rabatel et al. (2013), Schauwecker et al. (2017), Russell et al. (2017), Vuille et al. (2018a), and Yarleque

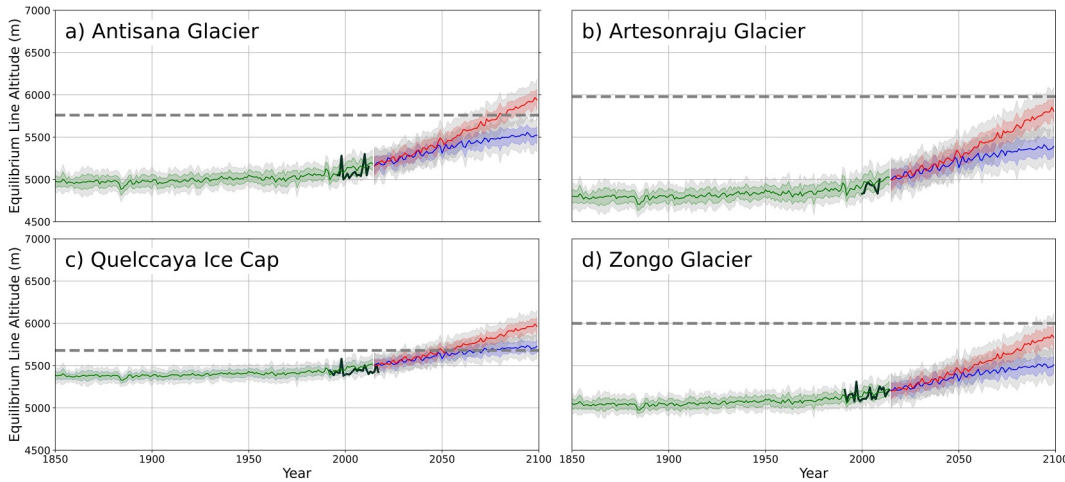

Figure 10. The annual-mean equilibrium-line altitude (ELA) at each location, including only the models which have an equilibrium climate sensitivity between 2.5°C and 4°C, for: (a) Antisana Glacier, (b) Artesonraju Glacier, (c) Quelccaya Ice Cap, and (d) Zongo Glacier. The CMIP6 historical multi-model mean is shown in green, ELA observations are plotted in black, the SSP2-4.5 multi-model mean is shown in blue, and the SSP5-8.5 scenario in red. The colored shading indicates ±1σ from the corresponding simulation's multi-model mean, and gray shading represents ±2σ from the multi-model mean. The dashed line indicates the highest altitude of the glacier at each location.

et al. (2018), although comparisons are hampered by the use of different time periods and reanalysis products across the various studies. The average FLH increase over the historical period documented in this study is also largely consistent with prior work. Bradley et al. (2009) found that the average FLH increase throughout the tropics was 10–20 m/decade from 1977 to 2007, which aligns well with the trends found in this study over the tropical Andes. Rabatel et al. (2013) looked at changes in the FLH from 1955 to 2011 over Antisana, the Cordillera Blanca, and Cordillera Real using NCEP/NCAR reanalysis. They showed an increase in FLH of 10.7 m/decade at Antisana, 28.9 m/decade at the Cordillera Blanca, and 27.1 m/decade at the Cordillera Real, which also lines up well with the results found using ERA5 in this study.

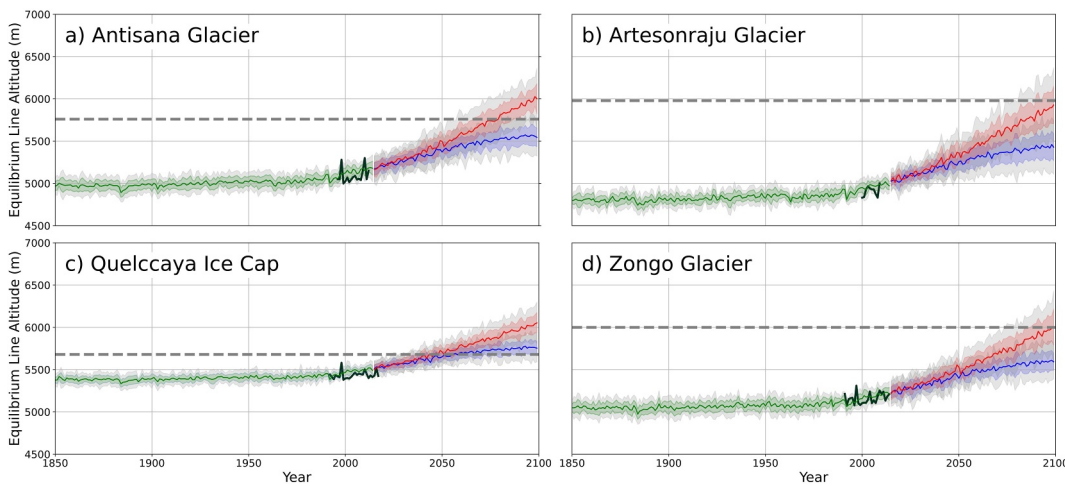

Figure 11. The annual-mean equilibrium-line altitude (ELA) at each location when considering only the "best-performing" models which have a bias of less than ±250 m and a difference in the interannual variability of less than 40 m compared with ERA5 for: (a) Antisana Glacier, (b) Artesonraju Glacier, (c) Quelccaya Ice Cap, and (d) Zongo Glacier. The CMIP6 historical multi-model mean is shown in green, ELA observations are plotted in black, the SSP2-4.5 multi-model mean is shown in blue, and the SSP5-8.5 scenario in red. The colored shading indicates ±1σ from the corresponding simulation's multi-model mean, and gray shading represents ±2σ from the multi-model mean. The dashed line indicates the highest altitude of the glacier at each location.

The observed FLH trends in ERA5 tend to be smaller than those simulated by CMIP6, although a meaningful comparison is difficult given that CMIP6 represents coupled models which cannot accurately capture the phasing of natural variability while reanalysis products represent a realistic realization of internal variability, such as the observed warm and cold phases of ENSO and the PDO, which significantly affected temperature trends in the Andes over the past decades (Vuille et al., 2015). Furthermore, when averaging across all CMIP6 models, internal variability is effectively canceled out and only external forcing remains.

In addition, our results also show that ERA5 in this region is warmer on average than the majority of the CMIP6 models used, with the average free-tropospheric temperatures of CMIP6 being significantly cooler than those of ERA5. Applying raw CMIP6 FLH estimates to derive Andean glacier ELA values, would thus inflate the projected lifespan of the investigated tropical glaciers. Applying a bias correction to the CMIP6 data is therefore critical to derive realistic estimates of future changes in FLH over the tropical Andes.

Strong correlations were found between the observed ELA and the ERA5 FLH at each of the four locations, documenting the significant empirical linear relationship that exists between these two variables. This relationship was employed to project ELA changes through the year 2100 using a large CMIP6 model ensemble as well as a subset of these models with a more consensus-based ECS between 2.5°C and 4°C and based on a model subset that performs the best over the historical period. Constraining the ECS reduces the model spread in the future ELA estimates and results in slightly lower ELA estimates. The differences between applying a basic bias correction and further constraining model choice based on their historical performance does not significantly change the outcome in most cases.

Based on our results, Antisana Glacier will likely persist through 2100 in the intermediate emission scenario, with all of the ECS-constrained and "best-performing" models placing the ELA below the maximum glacier elevation (Figure 12a). However, Antisana Glacier will likely lose its accumulation zone under SSP5-8.5. As shown in Figure 12a, the vast majority of bias-corrected, ECS-constrained, and "best-performing" models place the ELA above the peak of Antisana Glacier by 2100 under the SSP5-8.5 scenario. The outcome for Artesonraju and Zongo Glaciers is slightly more optimistic, as the multi-model mean shows a small accumulation zone persisting through 2100 in the low emission scenarios at both sites (Figures 12b and 12d). Under the high-emission scenario, the situation is more mixed. The multi-model mean ELA remains at or below the maximum glacier elevation at both sites, but there is a significant fraction of models which project an ELA above that critical elevation, especially for the bias-corrected and "best-performing" model subsets (Figures 12b and 12d). The slightly more optimistic outlook on Zongo and Artesonraju glaciers, when compared with Antisana, is primarily reflecting the higher elevation of those glaciers that extend up to ~6,000 m a.s.l., ensuring that a small accumulation zone may remain by the year 2100. Our results leave Quelccaya Ice Cap with the worst outcome out of the four mountain regions investigated. The accumulation zone will likely disappear in both scenarios, regardless of whether all models or only a subset of models is considered. Under the high emission scenario virtually all models project its disappearance (Figure 12c), with the ELA moving above the maximum elevation of the ice cap sometime after 2050. In the case of the SSP2-4.5 scenario, the bias-corrected, ECS-constrained and "best performing" multi-model means also all project the ELA to rise above the ice cap, but there are a few models where this is not the case (Figure 12c).

When looking more generally at the impact of bias-correcting, ECS-constraining, or selecting "best-performing" CMIP6 model subsets, it becomes apparent that each choice leads to a significant reduction in the uncertainty of future ELA projections as compared with a raw model application (Figure 12). Applying a bias correction or selecting the "best-performing" subset also leads to a higher end-of-century ELA when compared with ELA estimates using raw CMIP6 output, especially over the more southern glacier locations Zongo and Quelccaya. Constraining future estimates based on the models' ECS, on the other hand, further reduces the error estimate, especially for the SSP5-8.5 scenario, but it does not dramatically change the estimated ELA by the end of the 21st century, compared with the results using the full model envelope.

Finally Figure 12 also compares the results obtained in this study with earlier estimates based on CMIP5, published in Vuille et al. (2018) (Antisana, Artesonraju, and Zongo Glaciers) and Yarleque et al. (2018) (Quelccaya Ice Cap). However, this comparison needs to be made with caution as the results obtained in Vuille et al. (2018) and Yarleque et al. (2018) are based on a much smaller model ensemble (8 and 16 models, respectively), and rely on the older RCP scenarios used in CMIP5, which are slightly different from the SSP scenarios used in CMIP6. The RCP scenarios are similar to the SSP scenarios in that they both employ the same radiative forcing changes at the end of the century; however, SSP scenarios also provide socio-economic context to each scenario

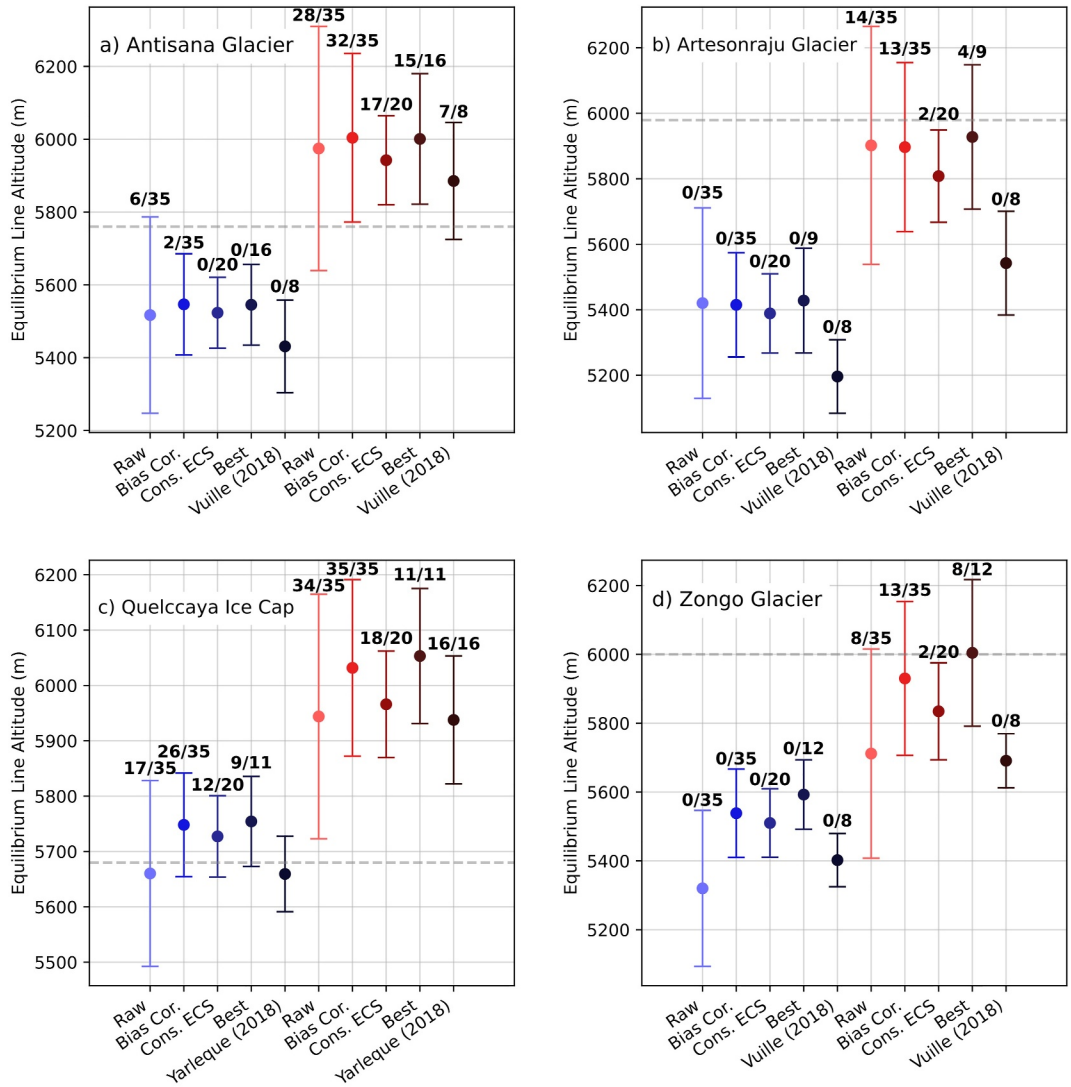

Figure 12. The multi-model mean (dot) equilibrium-line altitude (ELA) and one standard deviation away from the mean ELA (whiskers) for the year 2100 based on the raw CMIP6 data, bias-corrected CMIP6 data, ECS-constrained CMIP6 data, "best-performing" CMIP6 data, and CMIP5 data from Vuille et al. (2018) and Yarleque et al. (2018) for both SSP2-4.5 (shades of blue) and SSP5-8.5 scenarios (shades of red). The dashed horizontal line represents the highest glacier altitude at each location. The number above each bar indicates the fraction of models where the ELA is above the maximum glacier elevation by the year 2100. Note that the scale of *y*-axis varies across the four panels.

(IPCC, 2021). Also, the earlier studies used FLH estimates from two reanalysis data sets (ERA-Interim and NCEP/NCAR) to calculate ELA. As a result, the FLH-ELA slopes differ slightly between the studies (Table 4). Nonetheless, this comparison clearly documents that our new results put the ELA at a higher altitude by the end of the 21st century than the older estimates based on CMIP5. This result applies to both emission scenarios and is valid at all four locations, although the difference between CMIP5 and CMIP6 is most pronounced at Artesonraju and Zongo glaciers (Figure 12). The difference between the 2 model generations ranges from less than 50 m to more than 300 m, depending on location and scenario considered. It is further noteworthy that the older CMIP5 estimates published by Yarleque et al. (2018) indicated that Quelccaya might be able to retain a small accumulation zone by the end of the century under the RCP4.5 scenario. Our newer results suggest that Quelccaya will likely lose its entire accumulation zone even under this scenario.

Table 4
Comparison of r-Values and FLH-ELA Slopes Between This Study and Those Found in Vuille et al. (2018) for Antisana, Artesonraju, and Zongo Glaciers, and Yarleque et al. (2018) for Quelccaya Ice Cap

		Antisana	Artesonraju	Quelccaya	Zongo
r-value	Vuille et al. (2018)/Yarleque et al. (2018)	0.74	0.75	0.82	0.67
	This study	0.60	0.70	0.80	0.75
Slope (m/m)	Vuille et al. (2018)/Yarleque et al. (2018)	0.90	0.92	0.56	0.64
	This study	0.86	0.92	0.56	0.79

5. Summary and Conclusions

The primary motivation behind this study was to better constrain ELA projections in the tropical Andes region using the latest generation of GCM's, that is, CMIP6, to gain a better perspective on the lifetime and future extent of tropical Andean glaciers.

Our results highlight the importance of bias-correcting and constraining data from CMIP6 to obtain more accurate and useful information, as the ELA estimates based on uncorrected CMIP6 data reveal a wide range of outcomes than span a vertical ELA range of several hundred meters. This large uncertainty stems primarily from the strong dependence of future ELA estimates on the models' ECS and the models' ability to accurately simulate present-day conditions, which vary widely across the CMIP6 model generation.

While our study provides new and better constrained results of future ELA changes across a set of glaciers in the tropical Andes, our results broadly agree with those found in Vuille et al. (2018) and Yarleque et al. (2018). Glaciers located in the inner tropics, such as Antisana, will be exposed to the largest increase in the ELA. Indeed, Antisana Glacier is expected to continuously retreat and eventually disappear under a high-emission scenario and might persist as a very small glacier only in the intermediate emission scenario. The accumulation zones of Artesonraju and Zongo Glaciers on the other hand, have a better chance to persist through 2100, albeit in reduced size, although a small subset of models project their disappearance under a high emission scenario. This result is maybe not that surprising given that at both sites the mountains on which the glaciers are located are higher, reaching ∼6,000 m in both cases. In addition, subtropical glaciers, such as Zongo tend to be less sensitive to direct temperature changes and show a stronger dependence on changes in the hydrologic cycle, including early season snowfall (Autin et al., 2022). Finally, Quelccaya Ice Cap, due to the comparatively large ice mass and low maximum altitude, has different mechanics at play than the three other glaciers. The summit will likely enter the ablation zone of the glacier between 2050 (SSP5-8.5) and 2075 (SSP2-4.5), which only partially agrees with the findings of Yarleque et al. (2018), who had suggested that Quelccaya might be able to maintain a small accumulation zone under RCP4.5, based on their analysis of CMIP5 model results. Indeed the Quelccaya Ice Cap may persist into the 2100s as an ice-wasting remnant even in the new scenarios considered here, but it is destined to shrink until it will eventually disappear. Another factor to note for Quelccaya Ice Cap is the elevation feedback which will strengthen as the ice continues to thin out (Yarleque et al., 2018). As the ice cap thins, its maximum elevation will be lowered and the ice will thus be exposed to a warmer atmosphere and melt even faster (Bolibar et al., 2022). Such positive feedback mechanisms are not considered in our analysis; hence, our estimations of ELA changes throughout the 21st century are likely conservative.

The question arises as to whether the results presented here for a few glaciers can be generalized in terms of the future evolution of glaciers in the tropical Andes. Recent studies conducted at regional and global scales (e.g., Dussaillant et al., 2019; Caro et al., 2024; The Glambie Team, 2025) show that mass balances of tropical Andean glaciers are negative everywhere, and on the order of −0.5 m w.e./year over the first two decades of the 21st century. Of course, there is some spatial variability in mass losses, depending mainly on the maximum altitude reached by glaciers in the different glacierized cordilleras. Rabatel et al. (2013) had already shown that the annual mass loss rate of tropical Andean glaciers whose summit is below 5,400 m a.s.l. is twice as negative as that of glaciers whose maximum altitude is above this value, and in some places reaching over 6,000 m a.s.l., that is, allowing them to have a perennial accumulation zone. We show here that, for each of the four glacierized regions studied, which are distributed across the intertropical zone, the multi-model annual mean ELA will be over 5,800 m a.s.l. everywhere by the end of the 21st century. This necessarily implies a disappearance of glaciers whose entire surface lies below this limit, and a major reduction in the surface area of those whose maximum

altitude lies above it. As discussed in Vuille et al. (2018), there are additional limitations to our approach. This investigation relies solely on the empirical relationship between ELA and FLH, which is only one of the many factors of ELA change. While there is a strong correlation at each site between ELA and FLH, it does not explain all the changes seen in the ELA. Glacier surface mass balance is also a function of snow accumulation. To better estimate ELA changes, it is necessary to examine future changes in the hydrologic cycle at each of these locations. ELA changes are also dependent on various feedbacks not considered in this study, such as elevation-dependent warming and local ice-albedo feedbacks (Chimborazo et al., 2022; Magalhães et al., 2019; Pepin et al., 2022; Vuille et al., 2018). Investigating the effects of these feedbacks at each location would likely result in even better constrained ELA projections, but would require numerical downscaling of CMIP6 and reanalysis data sets, which was beyond the scope of this study.

Data Availability Statement

ERA5 reanalysis data are available at the ECMWF CDS (Hersbach et al., 2023). CMIP6 data are available at the Earth System Grid Federation (ESGF) model repository at https://aims2.llnl.gov/search/cmip6/. Glacier ELA data are available from the World Glacier Monitoring Service at WGMS (2025).

Acknowledgments
We are grateful for the comments from three anonymous reviewers who helped improve the quality and clarity of this manuscript. This study was supported by funding from NSF (OISE-1743738, EAR-2103041, and OISE-2412205).

References

Almazroui, M., Ashfaq, M., Islam, M. N., Rashid, I. U., Kamil, S., Abid, M. A., et al. (2021). Assessment of CMIP6 performance and projected temperature and precipitation changes Over South America. *Earth Systems and Environment*, *5*(2), 155–183. https://doi.org/10.1007/s41748-021-00233-6

Al-Yaari, A., Condom, T., Junquas, C., Rabatel, A., Ramseyer, V., Sicart, J.-E., et al. (2023). Climate variability and glacier evolution at selected sites across the world: Past trends and future projections. *Earth's Future*, *11*(10), e2023EF003618. https://doi.org/10.1029/2023EF003618

Autin, P., Sicart, J. E., Rabatel, A., Soruco, A., & Hock, R. (2022). Climate controls on the interseasonal and interannual variability of the surface mass and energy balances of a tropical glacier (Zongo Glacier, Bolivia, 16°S): New insights from the multi-year application of a distributed energy balance model. *Journal of Geophysical Research: Atmospheres*, *127*(7), e2021JD035410. https://doi.org/10.1029/2021JD035410

Baraer, M., Mark, B., McKenzie, J., Condom, T., Bury, J., Huh, K.-I., et al. (2012). Glacier recession and water resources in Peru's Cordillera Blanca. *Journal of Glaciology*, *58*(207), 134–150. https://doi.org/10.3189/2012JoG11J186

Basantes-Serrano, R., Rabatel, A., Francou, B., Vincent, C., Maisincho, L., Caceres, B., et al. (2016). Slight mass loss revealed by reanalyzing glacier mass-balance observations on Glaciar Antisana 15α (inner tropics) during the 1995–2012 period. *Journal of Glaciology*, *62*(231), 124–136. https://doi.org/10.1017/jog.2016.17

Basantes-Serrano, R., Rabatel, A., Francou, B., Vincent, C., Soruco, A., Condom, T., & Ruíz, J. C. (2022). New insights into the decadal variability in glacier volume of a tropical ice cap, Antisana (0 29 S, 78 09 W), explained by the morpho-topographic and climatic context. *The Cryosphere*, *16*(11), 4659–4677. https://doi.org/10.5194/tc-16-4659-2022

Birkel, S. D., Mayewski, P. A., Perry, L. B., Seimon, A., & Andrade-Flores, M. (2022). Evaluation of reanalysis temperature and precipitation for the Andean Altiplano and adjacent Cordilleras. *Earth and Space Science*, *9*(3), e2021EA001934. https://doi.org/10.1029/2021EA001934

Bolibar, J., Rabatel, A., Gouttevin, I., Zekollari, H., & Galiez, C. (2022). Nonlinear sensitivity of glacier mass balance to future climate change unveiled by deep learning. *Nature Communications*, *13*(1), 409. https://doi.org/10.1038/s41467-022-28033-0

Bradley, R. S., Keimig, F. T., Diaz, H. F., & Hardy, D. R. (2009). Recent changes in freezing level heights in the Tropics with implications for the deglacierization of high mountain regions. *Geophysical Research Letters*, *36*(17), L17701. https://doi.org/10.1029/2009GL037712

Bradley, R. S., Vuille, M., Diaz, H. F., & Vergara, W. (2006). Threats to water supplies in the tropical Andes. *Science*, *312*(5781), 1755–1756. https://doi.org/10.1126/science.1128087

Braun, M. H., Malz, P., Sommer, C., Farías-Barahona, D., Sauter, T., Casassa, G., et al. (2019). Constraining glacier elevation and mass changes in South America. *Nature Climate Change*, *9*(2), 130–136. https://doi.org/10.1038/s41558-018-0375-7

Bury, J. T., Mark, B. G., McKenzie, J. M., French, A., Baraer, M., Huh, K. I., et al. (2011). Glacier recession and human vulnerability in the Yanamarey watershed of the Cordillera Blanca, Peru. *Climatic Change*, *105*(1–2), 179–206. https://doi.org/10.1007/s10584-010-9870-1

Carey, M., Baraer, M., Mark, B. G., French, A., Bury, J., Young, K. R., & McKenzie, J. M. (2014). Toward hydro-social modeling: Merging human variables and the social sciences with climate-glacier runoff models (Santa River, Peru). *Journal of Hydrology*, *518*, 60–70. https://doi.org/10.1016/j.jhydrol.2013.11.006

Caro, A., Condom, T., Rabatel, A., Champollion, N., García, N., & Saavedra, F. (2024). Hydrological response of Andean catchments to recent glacier mass loss. *The Cryosphere*, *18*(5), 2487–2507. https://doi.org/10.5194/tc-18-2487-2024

Carrivick, J. L., Davies, M., Wilson, R., Davies, B. J., Gribbin, T., King, O., et al. (2024). Accelerating glacier area loss across the Andes since the Little Ice Age. *Geophysical Research Letters*, *51*(13), e2024GL109154. https://doi.org/10.1029/2024GL109154

Chimborazo, O., Minder, J. R., & Vuille, M. (2022). Observations and simulated mechanisms of elevation-dependent warming over the tropical Andes. *Journal of Climate*, *35*(3), 1021–1044. https://doi.org/10.1175/JCLI-D-21-0379.1

Chimborazo, O., & Vuille, M. (2021). Present-day climate and projected future temperature and precipitation changes in Ecuador. *Theoretical and Applied Climatology*, *143*(3–4), 1581–1597. https://doi.org/10.1007/s00704-020-03483-y

Drenkhan, F., Buytaert, W., Mackay, J. D., Barrand, N. E., Hannah, D. M., & Huggel, C. (2023). Looking beyond glaciers to understand mountain water security. *Nature Sustainability*, *6*(2), 130–138. https://doi.org/10.1038/s41893-022-00996-4

Drenkhan, F., Carey, M., Huggel, C., Seidel, J., & Ore, M. T. (2015). The changing water cycle: Climatic and socio-econiomic drivers of water-related changes in the Andes of Peru. *WIREs Water*, *2*(6), 715–733. https://doi.org/10.1002/wat2.1105

Dussaillant, I., Berthier, E., Brun, F., Masiokas, M., Hugonnet, R., Favier, V., et al. (2019). Two decades of glacier mass loss along the Andes. *Nature Geoscience*, *12*(10), 802–808. https://doi.org/10.1038/s41561-019-0432-5

Eyring, V., Bony, S., Meehl, G. A., Senior, C. A., Stevens, B., Stouffer, R. J., & Taylor, K. E. (2016). Overview of the Coupled Model Intercomparison Project Phase 6 (CMIP6) experimental design and organization. *Geoscientific Model Development*, *9*(5), 1937–1958. https://doi.org/10.5194/gmd-9-1937-2016

Favier, V., Wagnon, P., & Ribstein, P. (2004). Glaciers of the outer and inner tropics: A different behaviour but a common response to climatic forcing. *Geophysical Research Letters*, *31*(16), L16403. https://doi.org/10.1029/2004GL020654

Fernandez, A., & Mark, B. G. (2016). Modeling modern glacier response to climate changes along the Andes Cordillera: A multiscale review. *Journal of Advances in Modeling Earth Systems*, *8*(1), 467–495. https://doi.org/10.1002/2015MS000482

Francou, B., Vuille, M., Favier, V., & Cáceres, B. (2004). New evidence for an ENSO impact on low latitude glaciers: Antizana 15, Andes of Ecuador, 0°28'S. *Journal of Geophysical Research*, *109*(D18), D18106. https://doi.org/10.1029/2003JD004484

Gorin, A. L., Shakun, J. D., Jones, A. G., Kennedy, T. M., Marcott, S. A., Goehring, B. M., et al. (2004). Recent tropical Andean glacier retreat is unprecedented in the Holocene. *Science*, *385*(6708), 517–521. https://doi.org/10.1126/science.adg7546

Gualco, L. F., Maisincho, L., Villacís, M., Campozano, L., Favier, V., Ruiz-Hernández, J.-C., & Condom, T. (2022). Assessing the contribution of glacier melt to discharge in the tropics: The case of study of the Antisana glacier 12 in Ecuador. *Frontiers in Earth Science*, *10*, 732635. https://doi.org/10.3389/feart.2022.732635

Hausfather, Z., Marvel, K., Schmidt, G. A., Nielsen-Gammon, J. W., & Zelinka, M. (2022). Climate simulations: Recognize the 'hot model' problem. *Nature*, *605*(7908), 26–29. https://doi.org/10.1038/d41586-022-01192-2

Hersbach, H., Bell, B., Berrisford, P., Biavati, G., Horányi, A., Muñoz Sabater, J., et al. (2023). ERA5 monthly averaged data on pressure levels from 1940 to present. *Copernicus Climate Change Service (C3S) Climate Data Store (CDS)*. https://doi.org/10.24381/cds.6860a573

Ho, C. K., Stephenson, D. B., Collins, M., Ferro, C. A. T., & Brown, S. J. (2012). Calibration strategies: A source of additional uncertainty in climate change projections. *Bulletin of the American Meteorological Society*, *93*, 21–26. https://doi.org/10.1175/2011BAMS3110.1

Hugonnet, R., McNabb, R., Berthier, E., Menounos, B., Nuth, C., Girod, L., et al. (2021). Accelerated global glacier mass loss in the early twenty-first century. *Nature*, *592*(7856), 726–731. https://doi.org/10.1038/s41586-021-03436-z

Hurley, J. V., Vuille, M., Hardy, D. R., Burns, S. J., & Thompson, L. G. (2015). Cold air incursions, $\delta^{18}O$ variability, and monsoon dynamics associated with snow days at Quelccaya Ice Cap, Peru. *Journal of Geophysical Research: Atmospheres*, *120*(15), 7467–7487. https://doi.org/10.1002/2015JD023323

IPCC. (2021). Climate change 2021: The physical science basis. In V. Masson-Delmotte, P. Zhai, A. Pirani, S. L. Connors, C. Péan, et al. (Eds.), *Contribution of working group I to the sixth assessment report of the intergovernmental Panel on climate change* (p. 2391). Cambridge University Press. https://doi.org/10.1017/9781009157896

Kaser, G. (1999). A review of the modern fluctuations of tropical glaciers. *Global and Planetary Change*, *22*(1–4), 93–103. https://doi.org/10.1016/S0921-8181(99)00028-4

Kaser, G., Grosshauser, M., & Marzeion, B. (2010). Contribution potential of glaciers to water availability in different climate regimes. *Proceedings of the National Academy of Sciences*, *107*(47), 20223–20227. https://doi.org/10.1073/pnas.1008162107

LaFreniere, J., & Mark, B. G. (2014). A review of methods for estimating the contribution of glacial meltwater to total watershed discharge. *Progress in Physical Geography*, *38*(2), 173–200. https://doi.org/10.1177/0309133313516161

Magalhães, N. D., Evangelista, H., Condom, T., Rabatel, A., & Ginot, P. (2019). Amazonian biomass burning enhances tropical Andean glaciers melting. *Scientific Reports*, *9*(1), 16914. https://doi.org/10.1038/s41598-019-53284-1

Mark, B. G. (2007). Tracing tropical Andean glaciers over space and time: Some lessons and transdiciplinary implications. *Global and Planetary Change*, *60*(1–2), 101–114. https://doi.org/10.1016/j.gloplacha.2006.07.032

Mark, B. G., French, A., Baraer, M., Carey, M., Bury, J., Young, K. R., et al. (2017). Glacier loss and hydro-social risks in the Peruvian Andes. *Global and Planetary Change*, *159*, 61–76. https://doi.org/10.1016/j.gloplacha.2017.10.003

Meehl, G. A., Senior, C. A., Eyring, V., Flato, G., Lamarque, J., Stouffer, R. J., et al. (2020). Context for interpreting equilibrium climate sensitivity and transient climate response from the CMIP6 Earth system models. *Science Advances*, *6*(26), eaba1981. https://doi.org/10.1126/sciadv.aba1981

Meinshausen, M., Nicholls, Z. R. J., Lewis, J., Gidden, M. J., Vogel, E., Freund, M., et al. (2020). The shared socio-economic pathway (SSP) greenhouse gas concentrations and their extensions to 2500. *Geoscientific Model Development*, *13*(8), 3571–3605. https://doi.org/10.5194/gmd-13-3571-2020

Motschmann, A., Teutsch, C., Huggel, C., Seidel, J., Leon, C. D., Munoz, R., et al. (2022). Current and future water balance for coupled human-natural systems – Insights from a glacierized catchment in Peru. *Journal of Hydrology: Regional Studies*, *41*, 101063. https://doi.org/10.1016/j.ejrh.2022.101063

Pepin, N., Bradley, R. S., Dias, H. F., Baraer, M., Caceres, E. B., Forsythe, N., et al. (2015). Elevation-dependent warming in mountain regions of the world. *Nature Climate Change*, *5*, 424–430. https://doi.org/10.1038/nclimate2563

Pepin, N. C., Arnone, E., Gobiet, A., Haslinger, K., Kotlarski, S., Notarnicola, C., et al. (2022). Climate changes and their elevational patterns in the mountains of the world. *Reviews of Geophysics*, *60*(1), e2020RG000730. https://doi.org/10.1029/2020RG000730

Rabatel, A., Bermejo, A., Loarte, E., Soruco, A., Gomez, J., Leonardini, G., et al. (2012). Can the snowline be used as an indicator of the equilibrium line and mass balance for glaciers in the outer tropics? *Journal of Glaciology*, *58*(212), 1027–1036. https://doi.org/10.3189/2012JoG12J027

Rabatel, A., Francou, B., Soruco, A., Gomez, J., Cáceres, B., Ceballos, J. L., et al. (2013). Current state of glaciers in the tropical Andes: A multi-century perspective on glacier evolution and climate change. *The Cryosphere*, *7*(1), 81–102. https://doi.org/10.5194/tc-7-81-2013

Rangwala, I., & Miller, J. R. (2012). Climate change in mountains: A review of elevation-dependent warming and its possible causes. *Climatic Change*, *114*(3–4), 527–547. https://doi.org/10.1007/s10584-012-0419-3

Reveillet, M., Rabatel, A., Gillet-Chaulet, F., & Soruco, A. (2015). Simulations of changes to Glacier Zongo, Bolivia (16S), over the 21st century using a 3-D full-Stokes model and CMIP5 climate projections. *Annals of Glaciology*, *56*(70), 89–97. https://doi.org/10.3189/2015AoG70A113

Russell, A., Gnanadesikan, A., & Zaitchik, B. (2017). Are the central Andes Mountains a warming hot spot? *Journal of Climate*, *30*(10), 3589–3608. https://doi.org/10.1175/JCLI-D-16-0268.1

Saberi, L., McLaughlin, R. T., Ng, G. H. C., La Frenierre, J., Wickert, A. D., Baraer, M., et al. (2019). Multi-scale temporal variability in meltwater contributions in a tropical glacierized watershed. *Hydrology and Earth System Sciences*, *23*(1), 405–425. https://doi.org/10.5194/hess-23-405-2019

Schauwecker, S., Rohrer, M., Acuña, D., Cochachin, A., Dávila, L., Frey, H., et al. (2014). Climate trends and glacier retreat in the cordillera Blanca, Peru revisited. *Global and Planetary Change*, *119*, 85–97. https://doi.org/10.1016/j.gloplacha.2014.05.005

Schauwecker, S., Rohrer, M., Huggel, C., Endries, J., Montoya, N., Neukom, R., et al. (2017). The freezing level in the tropical Andes, Peru: An indicator for present and future glacier extents. *Journal of Geophysical Research: Atmospheres*, *122*(10), 5172–5189. https://doi.org/10.1002/2016JD025943

Seehaus, T., Malz, P., Sommer, C., Lippl, S., Cochachin, A., & Braun, M. (2019). Changes of the tropical glaciers throughout Peru between 2000 and 2016 – Mass balance and area fluctuations. *The Cryosphere*, *13*(10), 2537–2556. https://doi.org/10.5194/tc-13-2537-2019

Seehaus, T., Malz, P., Sommer, C., Soruco, A., Rabatel, A., & Braun, M. (2020). Mass balance and area changes of glaciers in the cordillera real and Tres Cruces, Bolivia, between 2000 and 2016. *Journal of Glaciology*, *66*(255), 124–136. https://doi.org/10.1017/jog.2019.94

Sicart, J. E., Hock, R., Ribstein, P., Litt, M., & Ramirez, E. (2011). Analysis of seasonal variations in mass balance and meltwater discharge of the tropical Zongo glacier by application of a distributed energy balance model. *Journal of Geophysical Research*, *116*(D13), D13105. https://doi.org/10.1029/2010JD015105

Sicart, J. E., Litt, M., Helgason, W., Tahar, V. B., & Chaperon, T. (2014). A study of the atmospheric surface layer and roughness lengths on the high-altitude tropical Zongo glacier, Bolivia. *Journal of Geophysical Research: Atmospheres*, *119*(7), 3793–3808. https://doi.org/10.1002/2013JD020615

Sicart, J. E., Wagnon, P., & Ribstein, P. (2005). Atmospheric controls of the heat balance of Zongo Glacier (16°S, Bolivia). *Journal of Geophysical Research*, *110*(D12), D12106. https://doi.org/10.1029/2004JD005732

Smith, C., Nicholls, Z. R. J., Armour, K., Collins, W., Forster, P., Meinshausen, M., et al. (2021). The Earth's energy budget, climate feedbacks, and climate sensitivity supplementary material. In V. Masson-Delmotte, P. Zhai, A. Pirani, S. L. Connors, C. Péan, S. Berger, et al. (Eds.), *Climate change 2021: The physical science basis. Contribution of working group I to the sixth assessment report of the intergovernmental panel on climate change*. Retrieved from https://www.ipcc.ch/

Somers, L. D., McKenzie, J. M., Mark, B. G., Lagos, P., Ng, G.-H. C., Wickert, A. D., et al. (2019). Groundwater buffers decreasing glacier melt in an Andean watershed—But not forever. *Geophysical Research Letters*, *46*(22), 13016–13026. https://doi.org/10.1029/2019GL084730

Soruco, A., Vincent, C., Rabatel, A., Francou, B., Thibert, E., Sicart, J. E., & Condom, T. (2015). Contribution of glacier runoff to water resources of La Paz city, Bolivia (16S). *Annals of Glaciology*, *56*(70), 147–154. https://doi.org/10.3189/2015AoG70A001

Taylor, L. S., Quincey, D. J., Smith, M. W., Potter, E. R., Castro, J., & Fyffe, C. L. (2022). Multi-decadal glacier area and mass balance change in the southern Peruvian Andes. *Frontiers in Earth Science*, *10*, 863933. https://doi.org/10.3389/feart.2022.863933

Urrutia, R., & Vuille, M. (2009). Climate change projections for the tropical Andes using a regional climate model: Temperature and precipitation simulations for the end of the 21st century. *Journal of Geophysical Research*, *114*(D2), D02108. https://doi.org/10.1029/2008JD011021

Voosen, P. (2022). Hot climate models exaggerate Earth impacts. *Science*, *376*(6594), 685. https://doi.org/10.1126/science.adc9453

Vuille, M., & Bradley, R. S. (2000). Mean annual trends and their vertical structure in the tropical Andes. *Geophysical Research Letters*, *27*(23), 3885–3888. https://doi.org/10.1029/2000GL011871

Vuille, M., Carey, M., Huggel, C., Buytaert, W., Rabatel, A., Jacobsen, D., et al. (2018). Rapid decline of snow and ice in the tropical Andes. Impacts, uncertainties and challenges ahead. *Earth-Science Reviews*, *176*, 195–213. https://doi.org/10.1016/j.earscirev.2017.09.019

Vuille, M., Francou, B., Wagnon, P., Juen, I., Kaser, G., Mark, B. G., & Bradley, R. S. (2008). Climate change and tropical Andean glaciers: Past, present, and future. *Earth-Science Reviews*, *89*(3–4), 79–96. https://doi.org/10.1016/j.earscirev.2008.04.002

Vuille, M., Franquist, E., Garreaud, R., Lavado Casimiro, W. S., & Cáceres, B. (2015). Impact of the global warming hiatus on Andean temperature. *Journal of Geophysical Research: Atmospheres*, *120*(9), 3745–3757. https://doi.org/10.1002/2015JD023126

Vuille, M., Kaser, G., & Juen, I. (2008). Glacier mass balance variability in the Cordillera Blanca, Peru and its relationship with climate and the large-scale circulation. *Global and Planetary Change*, *62*(1–2), 14–28. https://doi.org/10.1016/j.gloplacha.2007.11.003

Wagnon, P., Ribstein, P., Francou, B., & Sicart, J. E. (2001). Anomalous heat and mass budget of Glaciar Zongo, Bolivia, during the 1997-98 El Niño year. *Journal of Glaciology*, *47*(156), 21–28. https://doi.org/10.3189/172756501781832593

WGMS. (2025). Fluctuations of glaciers (FoG) database. *World Glacier Monitoring Service (WGMS), Zurich, Switzerland*. https://doi.org/10.5904/wgms-fog-2025-02b

Yarleque, C., Vuille, M., Hardy, D. R., Elison Timm, O., De la Cruz, J., Ramos, H., & Rabatel, A. (2018). Projections of the future disappearance of the Quelccaya Ice Cap in the central Andes. *Scientific Reports*, *8*(1), 15564. https://doi.org/10.1038/s41598-018-33698-z